ISAS - SCUOLA
INTERNAZIONALE
SUPERIORE
STUDI AVANZATI
TRIESTE
Strada Costiera 11

ISAS - INTERNATIONAL SCHOOL FOR ADVANCED STUDIES

THESIS FOR THE TITLE OF

"MAGISTER PHILOSOPHIAE"

A MOLECULAR DYNAMICS STUDY OF THE W(100) C(2X2) CLEAN SURFACE RECONSTRUCTION

Section: Physics of Condensed Matter

Supervisors: Prof. E.Tosatti and Prof. M.Parrinello

Candidate: Wang Cai-zhuang

Academic Year 1983/84

TRIESTE

A MOLECULAR DYNAMICS STUDY OF THE W(100) C(2X2) CLEAN SURFACE RECONSTRUCTION

WANG CAI-ZHUANG

International School for Advanced Studies (SISSA)

Trieste, Italy

This thesis is submitted for the degree of Magister of the International School for Advanced Studies in Trieste, Italy.

September 1984

ABSTRACT

We have performed a Molecular Dynamics study for the W(100) clean surface. The result shows a C(2X2) in-plane reconstruction at low temperature ($T < 200$ K) and a unreconstructed (1X1) structure at high temperature ($T > 200$ K).

CONTENTS

I. INTRODUCTION

The existence of clean-surface reconstruction of the surface W(100) and its behaviour with temperature, have been reported several years ago[1-4]. While LEED spots at the ideal surface reciprocal lattice points $(n, m)2\pi/a$ are observed at all temperature, an extra set of spots appears below $T_c \sim 300K$ at $(n, m)2\pi/a + (1/2,1/2)2\pi/a$. Thus the surface of W(100) undergoes a structural phase transition from (1 x 1) to commensurate C(2x2) structure as the temperature is lowered. A detailed analysis of the symmetry of LEED parterns has led Debe and King[3,4] to propose for W(100) clean-surface an asymmetric planar periodic distortion along <110> direction as shown in Fig. 1. The surface atom displacement was reported to be about $0.15 \sim 0.30$ $(1,1)(\pm 1/\sqrt{2})$ Å. This model is consistent with the observed lack of fourfold symmetry in the LEED parten[3,4] and has been accepted by most workers . However, Tsong and Sweeney[5] presented fully resolved atomic images of the W(100) plane obtained with a field-ion microscope at 21K showing no loss of the fourfold symmetry. Thus the precise nature of the low-temperature phase of W(100) surface has not been unquestionably determined.

It appears that this surface structural transformation depends on a lowering of the surface electronic energy, but the detailed mechanism is not completely understood. Estrup[1] and Tosatti[6,14] conjectured that half-filled surface state bands and ensuing surface charge-density-wave (SCDW) could be the driving force of the transition, as in an earlier model proposed for Si and Ge (111) by Tosatti and Anderson[7]. In this model the energy gain in the low temperature phase is produced by the displacement-induced rearrangement of the surface electrons just below E_F. When the two-dimensional Fermi line has parallel sections, a reconstruction

with wave vector spanning the two parallel sections leads to a gap at the Fermi line and a lowering of the total electronic energy. In general, this wave vector is incommensurate with the lattice, but when it is only slightly incommensurate, a commensurate structure can actually be lower in energy. This SCDW mechanism is compatible with the model proposed by Debe and King[3,4]. Several workers[8-11] have actually tried to study the energy of this phase change with somewhat contrasting results as to the importance of surface state electrons near the Fermi level. In particular, a negligible amount of surface nesting has been reported[12]. Eventually, only a "strong coupling CDW" can accounte for the reconstruction of W(100); for large distortions, the detailed periodicity is not dictated by the Fermi surface shape, but more by electronic considerations, a kind of band Jahn-Teller effect[13].

The surface reconstruction of W(100) seems to be second order phase transition and it is reversible on varying only the temperature. The conventional soft-mode approach to structural phase transition can be applied to obtain at least a mean-field description of this transition. When a structural phase transformation proceeds via a "soft-mode" instability, it is possible to represent the static distortions characterizing the structural rearrangements by a set of "frozen in" phononlike displacements. Tosatti[6,14] has noted that the parallel-shift model of Debe and King[3,4] exactly fits an $M_5(1,1)$ polarized phonon. Based on this viewpoint, a surface lattice dynamical approach to the reconstruction of W(100) has been performed by Fasolino, Santoro and Tosatti (FST)[15,16]. In this model they treat the reconstruction as an "effective" lattice phenomenon. Electrons are renormalized out, their driving effect being represented by extra forces between surface atoms. While a comprehensive treatment of the coupled electron-electron problem seems still beyound present possibilities, this lattice dynamical approach provide a realisitic description

of the T= 0 surface lattice distortion, and of its properties. This approach is also amenable to quantitative calculations. By analyzing the eigenmodes of a finite slab, tney showed that most observed transition on W(100) can be accounted for by an appropriate choice of surface force constant. The phase diagram they thus obtained is shown in Fig.2. However, the FST's lattice dynamical approach is limited to zero temperature and does not allow a study the temperature-dependent structural phase transition of W(100) surface. Morever, with FST's method, it is very difficult to determine the optimum force constant for the W(100) surface, because only static information can be used as input.

By introducing a microscopic lattice Hamiltonian, Ying and coworkers[13,17] have shown that it is possible to generate an temperature and coverage dependent effective lattice Hamiltonian for study of equilibrium phase transition properties of clean-surface and chemisorption system. Making further assumption that the reconstructions are strongly localized in the surface region, and the anharmonic effects can approximately limited entirely to the first layer, an effective two dimensional lattice Hamiltonian was also proposed[18] . With this approach, they have carried out Monte-carlo simulation and renormalizing group studies for W(100) and H/W(100) systems in more detail [13, 17, 18, 19].

In the present work, we follow the FST model. In order to overcome the difficulties in their method, we have performed a molecular dynamics study for the W(100) clean-surface. As is well known, the molecular dynamics (MD) method has become an important technique for the study of fluids and solids. Its remarkable seccess in the study of structural phase transition in the solids has been reported[20–25]. However, the MD method is applied here to the study of a surface reconstruction, to my knowledge, for the first time. In the FTS's model, the electrons is renormalized out and the system

is described by a lattice effective Hamiltonian which consists only the short range interaction between the Tungsten atoms. Thus such a system can be regarded as a classical system and is therefore suitable for our molecular dynamics study. With our MD method, what we have done here is

(1). Constructed and tested several potentials in order to obtain an optimum empirical pairwise potential for both bulk and surface Tungsten atoms.

(2). Characterized the surface structure of W(100) clean-surface at low temperature and high temperature.

(3). Studied the temprature-dependent structural phase transition of W(100) clean-surface. Because of our finite size, the actual critical region is not dealt with in any detail.

As we will see in the following, our MD method provited an useful tool for such investigations. In section II we will describe the MD method and its use in our simulation. The choice of potential is discussed in section III. The section IV show the results obtained in our MD simulation for the W(100) clean-surface. Finaly, some discussions are given in section V.

II. THE MOLECULAR DYNAMICS (MD) METHOD

Molecular dynamics (MD) is a method for studying classical statistical mechanics of well-defined systems through a numerical solution of Newton's equations. In a MD calculation a set of N classical particles have coordinates $\underline{r}_i$, velocities $\dot{\underline{r}}_i$ and masses m_i, i=1, ... ,N, are contained in a cell (MD cell) of volume V. The cell is generally cubic in shape. The particles are assumed to interact through some prescribed potential Vn ($\underline{r}_1 \cdots \underline{r}_N$) which in most investigation is taken to be pairwise.

$$V_n = \frac{1}{2} \sum_i \sum_j \phi(r_{ij}) \qquad (2.1)$$

where $r_{ij} = |\underline{r}_{ij}| = |\underline{r}_i - \underline{r}_j|$

Newton's equations are then

$$m_i \ddot{\underline{r}}_i = - \sum_{j \neq i} \frac{1}{r_{ij}} \frac{d\phi}{dr_{ij}} \underline{r}_{ij} \qquad i = 1, \cdots N \qquad (2.2)$$

These N coupled equations are solved numerically. For practical reason N is restricted to at most a few thousand and for small systems surface effects are obviously very important. In order to minimize the surface effects and to simulate more closely the properties of an infinite system a periodic boundary condition is almost invariably imposed.

In the standard MD method, the MD cell is fixed. As Vn being a function of r only, the total energy E of the system is conserved as the system moves along its trajectory. Thus the statistical ensemble generated in a conventional MD calculation is a (V, E, N) ensemble or microcanonical ensemble. The average of any property over the trajectory is an approximation to the measured value of that property for the thermodynamic state with the specified values of N, V and E, i.e. such an average is equivelent to an average over a microcanonical ensemble if the trajectory passes through all parts of phase space that have the specified energy.

With the MD method, not only the static quantities but also the

dynamic quantities can be obtained. This is one advantage over the Monte Carlo (MC) method. However, as in MC, the restriction that the MD cell be fixed in volume and shape restricts the applicability of the method, since the condition of the simulations are not the same as those normally encuntered in experiments (constant temperature, constant pressure or (T, P, N) conditions).

To perform the MD simulation at constant pressure, a modified MD method has been proposed by Anderson[26] . In his modified MD method, the volume of the MD cell becomes a variable and is allowed to fluctuation. The average volume is determined by the balance between the internal pressure and the externally set pressure. The trajectory averages for these type of simulation correspond to averages over the (H, P, N) ensemble.

However, in the method of Anderson, only changes in the volume of MD cell were possible but not in its shape. Thus crystal structure transformations are inhibited in Anderson's method because of the suppression of the essential fluctuation namely those in the shape of MD cell. In order to overcome the difficulty, Parrinello and Rahman (RP) have extended the ideal of Anderson to allow for changes of the MD cell shape[20,21] (This method is so called new MD method). The usefulness of new MD method has been demonstrated by applications to structural changes in the solid state[20-25].

Parallel to the constant pressure MD method, the constant temperature MD method has also been developed. To perform MD simulations at constant temperature, one can simply keep the kinetic energy constant by scaling the velocities at each time step[27,28]. In Anderson's paper[26], a method of controlling the velocity of the particles stochastically to produce the Boltzmann distribution was also proposed. More recently, Nose has

shown a MD method which can generate configurations belonging to the canonical (T, V, N) ensemble or the constant temperature constant pressure (T, P, N) ensemble.[33]

In our work, the MD method was used to test the bulk properties of the tungsten crystal and simulate the W(100) surface in order to study the surface reconstruction of that surface. The conditions at which we want to perform the MD simulation are either constant pressure or/and constant temperature corresponding to the following ensembles:

1. Constant pressure and constant temperature, i.e. (T,P,N)ensemble.
2. Constant pressure, i.e. (H,P,N) ensemble.
3. constant temperature, i.e. (T,V,N) ensemble.

To perform the MD simulation at constant pressure, the new MD method of Parrinello and Rahman has been employed. In the new MD the MD cell can have arbitrary shape and volume being completely described by three vectors $\underline{a}$, $\underline{b}$, and $\underline{c}$ that span the edges of the MD cell. The vector $\underline{a}$, $\underline{b}$ and $\underline{c}$ can have different lengths and arbitrary mutual orientations. An alternative description is obtained by arranging the vectors $\{\underline{a},\underline{b},\underline{c}\}$ to form a 3X3 matrix $\underline{\underline{h}}$ whose columns are, in order, the components of $\underline{a}$, $\underline{b}$, and $\underline{c}$. The volume is given by

$$V = \|\underline{\underline{h}}\| = \underline{a}\cdot(\underline{b}\times\underline{c}) \qquad (2.3)$$

The position $\underline{r}_i$ of a particle i can be written in terms of $\underline{\underline{h}}$ and of a column vector $\underline{s}_i$, with components s_i, η_i and ζ_i as

$$\underline{r}_i = \underline{\underline{h}}\,\underline{s}_i = s_i\underline{a} + \eta_i\underline{b} + \zeta_i\underline{c} \qquad (2.4)$$

where $0 \leq s_i, \eta_i, \zeta_i \leq 1$. In fact, we can think of s_i, η_i, ζ_i as the coordinates of the ith particle in a scaled MD cell. The images of $\underline{s}_i$ are at $\underline{s}_i + (\lambda, \mu, \nu)$ where λ, μ, ν are integers from $-\infty$ to $+\infty$. The square of the distance between i and j is given by

$$r_{ij}^2 = (\underline{s}_i - \underline{s}_j)^{\sim} \underline{\underline{G}} (\underline{s}_i - \underline{s}_j) \qquad (2.5)$$

where

$$\underline{\underline{G}} = \underline{\underline{h}}^{\sim} \underline{\underline{h}} \qquad (2.6)$$

The reciprocal space is spanned by the vectors

$$\frac{2\pi}{V}(\underline{b}\times\underline{c}, \underline{c}\times\underline{a}, \underline{a}\times\underline{b}) = \frac{2\pi}{V}\underline{\underline{\sigma}} \qquad (2.7)$$

The matrix $\underline{\underline{\sigma}} = V(\underline{\underline{h}}^{\sim})^{-1}$ carries information concerning the size and orientation of the MD cell.

In the case where only hydrostatic pressure is applied, the 3N dynamical variables that describe the possitions of the N particles were augemented by the nine components of $\underline{\underline{h}}$. The time evolution of the 3N+9 variables was then obtaied from the Lagrangian

$$\mathcal{L} = \frac{1}{2}\sum_{i=1}^{N} m_i \dot{\underline{s}}_i^{\sim} \underline{\underline{G}} \dot{\underline{s}}_i - \sum_{i=1}^{N}\sum_{j>i}^{N} \phi(r_{ij}) + \frac{1}{2} w \, Tr\, \dot{\underline{\underline{h}}}^{\sim} \dot{\underline{\underline{h}}} - PV \qquad (2.8)$$

where P denotes the externally applied hydrostatic pressure, $\phi(r)$ is the pair potential, the kinetic term assoc iated with the time variation of $\underline{\underline{h}}$ has a constant of proportionality w which has the dimension of mass. As it has been pointed out by Parrinello and Rahman, the Lagrangian (2.8) generates an isoenthalpic-isobaric ensemble, apart from a small correction arising from the term in w.

From (2.8) the lagrangian equations of motion are easily written down

$$\ddot{\underline{s}}_i = -\sum_{j\neq i} m_i^{-1}\left(\frac{\phi'}{r_{ij}}\right)(\underline{s}_i - \underline{s}_j) - \underline{\underline{G}}^{-1}\dot{\underline{\underline{G}}}\,\dot{\underline{s}}_i \qquad i = 1, \cdots N \qquad (2.9)$$

$$w\dot{\underline{\underline{h}}} = (\underline{\underline{\Pi}} - P)\underline{\underline{\sigma}} \qquad (2.10)$$

where, using the usual dyadic notation and writing $\underline{v}_i = \underline{\underline{h}}\,\dot{\underline{s}}_i$

$$V\underline{\underline{\Pi}} = \sum_i m_i \underline{v}_i \underline{v}_i - \sum_i \sum_{j>i} \left(\frac{\phi'}{r_{ij}}\right) \underline{r}_{ij}\,\underline{r}_{ij} \qquad (2.11)$$

Note that for the special case of $\underline{\underline{h}}$ =constant, i.e. when the MD cell

is fixed in volume and shape, $\dot{\underset{\sim}{G}} = 0$ and due to Eq.(2.4), Eq.(2.9) becomes identical to Eq.(2.2). Thus the formulas established in the new MD method as described above can also be used for the simulation of standard (E,N,V) ensemble, simply setting $\underset{\sim}{h}$ =constant.

For the constant temperature MD simulation we have used the method proposed by Anderson[26]. We pick an initial set of positions and velocities $r_i(0)$ and $v_i(0)$, and integrate the equations of motion. At every ten MD steps, each particle is supposed to suffer a collision. Each collision is an instantaneous event that affect the velocity of one particle. The value of the velocity of particle i after the collision is chosen at random according to the following function

$$\frac{v_i}{\sqrt{mT}} = \cos(2\pi R_i) \times \sqrt{(-2) \times \log R_i'}, \quad i = 1, \cdots N \qquad (2.12)$$

where R_i and R_i' are the random numbers between 0 and 1, to generate Boltzmann distribution of velocity of the particles coresponding to temperature T. Then the equations of motion for the entire collection of particles are intergrated again. This process is repeated. In what follows we will call this way of controlling the temperature as the "canonical temperature control.

As it has been pointed out by Anderson, the result of this constant temperature MD procedure is a trajectory, specified by $\underset{\sim}{r}_i(t)$ and $\underset{\sim}{p}_i(t)$ for N particles in a volume V with periodic boundary conditions and the average of any function $F(\underset{\sim}{r}_i, \underset{\sim}{p}_i, V)$ over this trajectory is equal to the ensemble average of F for the canonical ensemble in which the temperature is T.

In MD simulations, it frequently happens that one want to "heat" or "cool" the system in order to study the behaviour of the system with temperature. As the temperature changes, the energy of the system changes from one energy shell to another. Since the temperature of the system is obtained by averaging the kinetic energy of the particles, one can easily

change the temperature by multiplying the velocity of the particles by a factor α ($\alpha > 1$ for heating, $\alpha < 1$ for cooling). The choice of α and the frequency with which it is applied will vary according to circumstances.

In our calculation, the MD cell is formed by arranging a set of particles in a B.C.C. lattice with the W lattice parameter $a_o = 3.16$ Å . By imposing the periodic boundary condition along x, y, z, i.e. in three dimensions, we simulate the bulk properties, while imposing periodic boundary condition along x, y only, we obtain a n-layer slab, which can be used to study the surface properties.

The algorithm we adopted to integrate the equations of motion is the fifth order predictor-corrector algorithm. Let us denote any given cartesian component of $\underset{\sim}{r}_i(t)$ by q_o, of $\dot{\underset{\sim}{r}}_i(t)\,\Delta t$ by q_1, of $\ddot{\underset{\sim}{r}}_i(t)(\Delta t)^2/2!$ by q_2 and so on. Using a Tayler expansion it is possible to predict the values of all the derivatives of the positions at $t+\Delta t$. Denoting the predicted values of q_i by P_i , one obtains

$$
\begin{aligned}
P_0 &= q_0 + q_1 + q_2 + q_3 + q_4 + q_5 \\
P_1 &= q_1 + 2q_2 + 3q_3 + 4q_4 + 5q_5 \\
P_2 &= q_2 + 3q_3 + 6q_4 + 10q_5 \\
P_3 &= q_3 + 4q_4 + 10q_5 \\
P_4 &= q_4 + 5q_5 \\
P_5 &= q_5
\end{aligned}
\qquad (2.13)
$$

Hense from P_2 we can get the predicted value of the acceleration at $t+\Delta t$.

Using P_o, which are the predicted positions at $t+\Delta t$ the accelerations in predicted positions can be calculated using the equations of motion. Let $a(P_o)$ denote these accelerations and $\tilde{P}_2$ denote $a(P_o)(\Delta t)^2/2$ the difference $D = \tilde{P}_2 - P_2$ allows us to get corrected values C_i from the predicted values P_i as follows

$$C_i = P_i + f_{i2}^{(5)} D \qquad i = 0,1, \ldots,5 \qquad (2.15)$$

where the numbers $f_{i2}^{(5)}$ are 3/16, 251/ 360, 1, 11/ 18, 1/6, 1/60 respectively for i = 0,1,2,3,4,5.

By solving the equations of motion we get all $\underset{\sim}{r}_i(t)$ and their derivatives at each time t. Then any thermodynamical or structural quantities Q at that time can be evaluated. The accutate static value of that Q is then obtained by averaging Q(t) at equilibrium for a sufficient number of steps. In particular, the following quantities have been calculated in our similation ; in order to characterize the properties of the W-bulk and W(100) surface.

(1). THE ENERGY

From the Lagrangian Eq.(2.8) one can construct the corresponding Hamiltonian following the usual rules of mechanics. Since the system is not subject to time dependent external forces, this is a constant of motion. We get

$$\mathcal{H} = \sum_i \tfrac{1}{2} m_i v_i^2 + \tfrac{1}{2} \sum_i \sum_j{}' \Phi(r_{ij}) + \tfrac{1}{2} w T_r \dot{\underset{\sim}{h}}^{\sim} \dot{\underset{\sim}{h}} + PV \qquad (2.16)$$

In the case of fixed MD cell and if we set P = 0, then (2.16) simply gives

$$\mathcal{H} = \sum_i \tfrac{1}{2} m_i v_i^2 + \tfrac{1}{2} \sum_i \sum_j{}' \Phi(r_{ij}) \qquad (2.17)$$

The energy of the system is then obtained by

$$E = \langle \mathcal{H} \rangle \qquad (2.18)$$

Performing the average over sufficient number of MD steps at equilibrium, it will give the energy with sufficient accuracy.

We can also rewrite the Hamiltonian (2.17) as

$$\mathcal{H} = \sum_i \left(\tfrac{1}{2} m_i v_i^2 + \tfrac{1}{2} \sum_j{}' \Phi(r_{ij}) \right) = \sum_i \varepsilon_i \qquad (2.19)$$

with

$$\varepsilon_i = \tfrac{1}{2} m_i v_i^2 + \tfrac{1}{2} \sum_j{}' \Phi(r_{ij}) \qquad (2.20)$$

Then

$$E = \langle \mathcal{H} \rangle = \langle \sum_i \varepsilon_i \rangle = \sum_i \langle \varepsilon_i \rangle \qquad (2.21)$$

here ε_i and $\langle \varepsilon_i \rangle$ are the Hamiltonian and energy of ith particle in the case of fixed MD cell respectively. It is obviously that ε_i and $\langle \varepsilon_i \rangle$ can be evaluated in our MD simulation. So in addition to the total energy of the system we can also obtain the contribution of energy from each particle as well as from each atomic layer.

For the porpose of investigation of surface phase transition, we have defined the surface Hamiltonian and surface energy as

$$\mathcal{H}_s = \sum_l \varepsilon_l \quad ; \quad E_s = \langle \mathcal{H}_s \rangle = \sum_l \langle \varepsilon_l \rangle \qquad (2.22)$$

where l runs over all the surface atoms. Another energy we call it surface interlayer energy defined through

$$E_s' = \langle \sum_l \frac{1}{2} m_l v_l^2 + \frac{1}{2} \sum_l \sum_{l'}' V^{surf}(r_l - r_{l'}) \rangle \qquad (2.23)$$

has also been evaluated. Where the l in the first sum runs over all surface atoms and l,l' in the second sum run over pairs of first neighbour atoms in the surface layer.

(2). The structural quantities

In our work the structure of the system was recongnized by calculating the pair correlation function g(r) and the static structure factor S(K). Both the bulk g(r) and the $g^s(r)$, the pair correlation function for the surface layer, are calculated. The structure factor S(K) is calculated only for the surface layer. Besides, the average coordinates of the particles with respect to their ideal B.C.C. lattice (ideal square lattice in the (100) surface) are evaluated, which has been ploted out to give a visual impression of the structure of the system.

The standard method was used to carry out the pair correlation functions. A sphere having radis r_{max} in real space was devided into shells of thickness Δr. At each MD step or after several MD steps the distribution

of the particles is counted for each shell. After long time average at equilibrium the distribution of the particles among the shells will give the pair correlation function $g(r)$ for $0 \leq r \leq r_{max}$. In fact, in order to avoid the square root calculation for saving computer time, in the MD program the variable used is r^2 rather than r itself. Hoever, the calculated $g(r^2) \sim r^2$ is easily transformed into $g(r) \sim r$.

The structure factor S(K) was defined as

$$S(K) = \frac{1}{N_s} \left| \sum_{l} e^{-i K \cdot r_{\parallel l}} \right|^2 \qquad (2.24)$$

where l runs over all N_s surface layer atoms, $r_{\parallel l}$ the components of r_l parallel to the surface, k is also a wave vector parallel to the surface. In our calculation, S(K) was evaluated for the set of K points in first Brillouin zone of W(100) surface.

(3). The specific heat

In order to study the phase transition of W(100) surface reconstruction, we have tried to evaluate the specific heat of the system. The common method by means of energy fluctuation was used to evaluate such a quantity. If we perform the MD simulation at constant temperature (T,V,N) ensemble, this simply gives

$$C_v = \frac{\langle \mathcal{H}^2 \rangle - \langle \mathcal{H} \rangle^2}{k_B T^2} \qquad (2.25)$$

However, the contribution from bulk atoms to C_v dominate that one coming from the surface atoms. Since the surface reconstruction affects mainly the surface layer, we are interested also singling out the contribution of the surface atoms to C_v. We shall refer to this contribution as the surface specific heat C_v^s.

Following the classical statistical mechanics, the average surface energy Es can be calculated as

$$E_s = \langle \mathcal{H}_s \rangle = \frac{\int dp\, dq\, \mathcal{H}_s\, e^{-\beta \mathcal{H}}}{\int dp\, dq\, e^{-\beta \mathcal{H}}} \qquad (2.26)$$

Hence

$$\int dp\, dq\, [E_s - \mathcal{H}_s(P,Q)]\, e^{\beta[A(V,T) - \mathcal{H}(P,Q)]} = 0 \qquad (2.27)$$

here A(V,T) is the free energy of the system.

Differentiating both sides with respect to β we obtain

$$\frac{\partial E_s}{\partial \beta} + \int dp\, dq\, e^{\beta(A-\mathcal{H})} (E_s - \mathcal{H}_s)(E - \mathcal{H}) = 0 \qquad (2.28)$$

i.e.

$$k_B T^2 \frac{\partial E_s}{\partial T} = \langle (\mathcal{H}_s - E_s)(\mathcal{H} - E) \rangle \qquad (2.29)$$

Therefore the surface specific heat C_v^s is given by

$$C_v^s = \frac{\partial E_s}{\partial T} = \frac{\langle (\mathcal{H}_s - E_s)(\mathcal{H} - E) \rangle}{k_B T^2} \qquad (2.30)$$

III. CHOICE OF THE POTENTIAL

The superlattice distortion on W surface is believed as the two-dimensional equivalent of a ferroelectric distortion, or of a Peierls-type distortion of the kind observed in layered structures and in quasi-one dimensional metals[29-31]. The driving force for the structural transition on the W surface must , strictly speaking, be electronic in nature. As has been pointed out by FST[16], in such a "strong coupling" structural phase transition, most detail of the periodic lattice distortion as well as of the thermodynamics of the transition can be understood solely in lattice dynamical terms. In particular the role of the electrons can be lumped into a suitable short-range force, and the electron entropy can be totally neglected. Because of the short-ranged nature of the interactions, an

effective lattice Hamiltonian is useful for the strong coupling transition .

Following the FST[15,16], we introduce an effective lattice Hamiltonian

$$\mathcal{H} = \sum_R \frac{P_R^2}{2m} + \frac{1}{2}\sum_{(\vec{R},\vec{R}')} V^{bulk}(\vec{R}-\vec{R}') + \frac{1}{2}\sum_{\langle \vec{R},\vec{R}'\rangle} V^{surf}(\vec{R}-\vec{R}') \qquad (3.1)$$

where $\vec{R}$, $\vec{R}'$ denote W atoms at the lattice sites of a slab. The first double sum $(\vec{R}\vec{R}')$ extends to all $\vec{R},\vec{R}'$ that are either first or second neighbours and not on the same surface. The second double sum $\langle \vec{R},\vec{R}'\rangle$ extends over all $\vec{R}$, $\vec{R}'$ that are first neighbours on the same surface. The scope of this distinction is to allow for a different type of interaction between surface neighbours and bulk neighbours, as required by the existence of half-filled surface states in the former case.

The bulk potential $V^{bulk}(R)$ consists of two essential parts $V_1(R)$ and $V_2(R)$ which describe the interactions between the first neighbours and second neighbours respectively. Both $V_1(R)$ and $V_2(R)$ are taken in the form of an expansion to the fourth order about their own equilibrium positions (for Tungsten the second neighbour distance a_o= 3.16 A, the first neighbour distance $a_1 = a_o/\sqrt{2}$).

$$V_1(R) = V_{10} + \alpha_1 a_1 (R-a_1) + \frac{1}{2!}\beta_1 (R-a_1)^2 + \frac{1}{3!a_1}\gamma_1 (R-a_1)^3 + \frac{1}{4!a_1^2}\delta_1 (R-a_1)^4$$

$$V_2(R) = V_{20} + \alpha_2 a_o (R-a_o) + \frac{1}{2!}\beta_2 (R-a_o)^2 + \frac{1}{3!a_o}\gamma_2 (R-a_o)^3 + \frac{1}{4!a_o^2}\delta_2 (R-a_o)^4 \qquad (3.2)$$

where V_{1o} and V_{2o} are some constant describing the strength of the bulk potential. $\alpha_1, \beta_1, \gamma_1, \delta_1$ and $\alpha_2, \beta_2, \gamma_2, \delta_2$ are the force constant. Since a first-priciples calculation of these quatities still seems not avalible at present, we treat them as free parameters and adjust them to fix the known harmonic and anharmonic properties of the bulk Tungsten.

V_{1o} and V_{2o} are chosen in order to satisfy the relation

$$\frac{1}{2N}\sum_{(\vec{R}_o,\vec{R}'_o)} V^{bulk}(\vec{R}_o-\vec{R}'_o) = 3V_{1o} + 4V_{2o} = 8.66\,ev \qquad (3.3)$$

where 8.66ev is the cohesive energy(per atom) of the B.C.C. Tungsten, $\vec{R}_o$ and $\vec{R}'_o$ are the equilibrium position of the atoms. the harmonic part of force constant $\alpha_1, \beta_1, \alpha_2, \beta_2$ are taken from the work of Castiel et al[32] in which they have shown that these parameters reproduce well the experimental phonon spectum of the bulk Tungsten. The unharmonic force constants $\gamma_1, \delta_1, \gamma_2, \delta_2$ are then chosen in some arbitrary manner and adjusted, as far as we can, to give reasonable thermal expansion compared to experiment. We also require the constructed bulk potential should give a stable B.C.C. structure in the MD simulations.

In our work, two kinds of bulk potential constructed in different ways have been studied. One of such potentials was constructed in the form as show in Fig.3.1, which corresponds to the following set of parameters

V_{1o}= -1.2545 ev , V_{2o}= -1.2139 ev

α_1 = -0.04 $THz^2 g$, β_1 = 6.11 $THz^2 g$, γ_1 = -124.0 $THz^2 g$, δ_1 = 696.4 $THz^2 g$,

α_2 = 0.04 $THz^2 g$, β_2 = 4.37 $THz^2 g$, γ_2 = -105.2 $THz^2 g$, δ_2 =6330.5 $THz^2 g$.

In this potential the conection between the two parabolic parts $V_1(R)$ and $V_2(R)$ is smoothed by giving an energy barrier between the first neighbour and second neighbour distance. In the following we denote this bulk potential as "BP-A".

The bulk potential "BP-A" was tested in our MD simulation for bulk W before using it for the surface investigations. The simulation was perfored at constant pressure using the new MD method described in section II. The results have shown that this potential keeps well the B.C.C. structure of W crystal. The corresponding pair-correlation functions obtainted are shown in Fig. 3.2. However, the thermal expansion of the lattice with this potential is not good compare to the experiment (see Fig. 3.3). As we will

see in the following section, further use of this potential in the lattice Hamiltonian(3.1) for the surface study show that the surface structure change with temperature is irreversible with this potential. However,since a lot of our work has been carried out with this potential and the results from this work did give us some useful informations for the understanding of the problem, we would like to spend some space in our thesis on it despite its defects.

In order to overcome the defects in the previous bulk potential "BP-A", we have constructed another bulk potential in the form shown in Fig. 3.1(b). In this construction, the first neighbour potential $V_1(R)$ and second neighbour potential $V_2(R)$ are taken in the parabolic form respectively, and we din't try to construct a single potential by joining them as we did in constructing "BP-A". If two atoms are first neighbour at T=0K,they interact with $V_1(R)$; while if they are second neighbours , they interact with $V_2(R)$. The bulk potential shown in Fig. 3.1(b) corresponds to the following parameters

$$V_{1o} = -1.2545 \text{ ev} \quad , \qquad V_{2o} = -1.2139 \text{ ev}$$

$$\alpha_1 = -0.04 \text{ THz}^2 g, \quad \beta_1 = 6.11 \text{ THz}^2 g, \quad \gamma_1 = -124.0 \text{ THz}^2 g, \quad \delta_1 = 4000 \text{ THz}^2 g,$$

$$\alpha_2 = 0.40 \text{ THz}^2 g, \quad \beta_2 = 4.37 \text{ THz}^2 g, \quad \gamma_2 = -105.0 \text{ THz}^2 g, \quad \delta_2 = 2000 \text{ THz}^2 g.$$

and we shall denote this bulk potential as "BP-B".

Although the form of the new bulk potential "BP-B" seems unusual in contrast to the most pairwise potentials, it has desirable properties over that of the previous potential "BP-A". It has been checked by our MD simulation that with the bulk potential "BP-A", the jumping probbility of the first neighbour atom over the energy barrier to the second neighbour was found to be large, even at low temperature. In order to eliminate this unphysical jumping, a higher energy barrier is required, if we adopt the bulk potential in the form of " "BP-A". However, experimental data on thermal expansion and phonon spectum imposes a certain limitation on the choice of the force constants in the potential and it is impossible to introduce such a high energy barrier. If we adopt the bulk potential in the form of "BP-B", this difficulty can be overcome

automatically. Moreover, the separate potentials $V_1(R)$ and $V_2(R)$ are expected to give a better description of the strong chemical bonds among the first neighbour atoms and the second neighbour atoms respectively.

A test of the potential "BP-B" in our constant pressure MD simulation for bulk W has shown that this potential gives a stable B.C.C. structure. The corresponding pair correlation functions shown in Fig. 3.4 indicate that the system remained in B.C.C. structure at the temperature as high as to T=3000K. In contrast to the case of the previous potential "BP-A", the thermal expansion given by this potential is in good agreement with experiment at least for $0 \leq T \leq 2500$K (see Fig.3.5). As we shall see in the following section the use of "BP-B" in the investigation of W(100) surface gives desirable reversibility of the surface structure with the temperature T.

It has been noted that the system does not show proper expansion at high temperature above 3000 K(see Fig. 3.5). The main reason for this is that in "BP-B", both $V_1(R)$ and $V_2(R)$ have a tail too steep for large R compared to the exponential behaviour of most of usual pairwise potentials. In order to improve the situation, higher order terms will have to be included in the expansion of the potential of Eq.(3.2) and these will be more free parameters which makes the situation more complicated.Since in the present study of surface reconstruction we are interested mainly only in the temperature range $0 \leq T \leq 1000$K, the potential "BP-B" is expected to be suitable for the present porpose.

The surface potential $V^{surf}(R)$ is also given as a simple expansion

$$V^{surf}(R) = V_{s0} + \alpha_s a_0 (R-a_0) + \frac{1}{2!}\beta_s (R-a_0)^2 + \frac{1}{3!a_0}\gamma_s (R-a_0)^3 + \frac{1}{4!a_0^2}\delta_s (R-a_0)^4 \qquad (3.4)$$

about the ideal surface neighbour distance a_0(=3.16 A for W). Here α_s, β_s and γ_s, δ_s are free parameters controlling the harmonic and anharmonic parts of the potential respectively. At present, our knowledge about the surface

force constants of W(100), especially the anharmonic part, is not yet detailed enough. In our work, these parameters are chosen from the Slab lattice dynamical results of Fasolino. In the slab lattice dynamics, this set of parameters gives an unstable M_5 mode on the ideal 1x1 surface and a stable phonon spectum for the C(2x2) reconstructed surface with an in-plane distortion of reasonable amplitude.

Three surface potentials have been used in the lattice Hamiltonian(3.1) for the study of W(100) surface reconstruction. They correspond to the following parameters respectively

Potential	α_s THz^2g	β_s THz^2g	γ_s THz^2g	δ_s THz^2g	V_{so} ev	
SP-1	-0.66	-1.215	5.0	500.0	0.7639	See Fig3.1
SP-2	-0.66	-1.215	5.0	500.0	0.8868	See Fig3.1
SP-3	-1.30	-0.700	10.0	500.0	1.8000	See Fig3.1

Note that in SP-2 and SP-3 the V_{so} has been adjusted so as to give a totally repulsive $V^{surf}(R)$.

Finally, in order to have a stable reconstructed surface with non-zero distortion d along <1,1> direction as that in Fig. 1 , the combination of bulk and surface potentials in the lattice Hamiltonian (3.1) must show a minimum energy for $d \neq 0$ at T=0. In the Fig. 3.6 and Fig. 3.7 we show the E~d curve at T=0 K obtained by using the potentials "BP-A"+"SP-1"(on one surface) and "BP-B"+"SP-3"(on one surface) respectively. The effects of the surface relaxation ΔZ was also considered in the figures. For the Hamiltonian with "BP-A"+"SP-1" the equilibrium at T = 0K was found at $d \approx 0.17$ A, $\Delta Z \approx 0.04$ A, while for the Hamiltonian with "BP-B"+"SP-3", $d \approx 0.15$ A and $\Delta Z = 0.02$ A was found to be the most stable configuration at T=0K.

IV. THE RESULTS

In the simulation of W(001) surface, our MD cell consists of either 128 or 512 particles. The particles were arranged in B.C.C. structure with lattice parameter of W (a=3.16A). The MD cell of 128 atoms contains 4x4 unit cell in the X-Y plane and 8 atomic layers along the Z direction(we shall call this sample as 4x4 sample), while the MD cell of 512 atoms has 8x8 unit cell in X-Y plane and 8 atomic layers along the Z direction(we shall call this sample as 8x8 sample). By imposing the periodic boundary condition along X,Y direction , we obtain an eight layer slab with two W(001) surfaces. The atoms interact with each other through the potential $\phi(r)$ as described in the Section III. In our simulation, the surface potential may be imposed on two surfaces(both top and bottom surface) or imposed on top surface only, depending on the simulating condition required. In the simulation, we have chosen ev as the unit of energy, A as that of length and the mass of tungsten atom as that of mass. Then the unit of time is given by

$$\left(\frac{[m][L]^2}{[E]}\right)^{1/2} \approx 1.38 \times 10^{-13}\text{sec.}$$

The simulation was started either from the unreconstructed (1x1)structure or reconstructed C(2X2) structure on the surface. In both cases, the bulk structure was kept as B.C.C. A small random displacement of the particles from the initial positions and zero velocities provided the conditions for the ensuring dynamics. With the time step t=0.02 unit, the fifth order perdictor-corrector algorithm was used to integrate the equations of motion (2.9) and (2.10). The canonical temperature control method was used to perform the simulation at constant temperature. In the simulation of (T,V,N) ensemble, the MD cell was fixed at given temperture and was expanded uniformly according to the experimental thermal expansion data as the temperature changed. At the constant pressure simulation, the external pressure was set

to zero. The simulations were performed for various temperatures. At each temperature, after a long period of "aging" to allow for establishment of equilibrium, an averaging procedure over 2000 time units followed to evaluate the physical quantities concerned, as described in Sec.II.

Throughout, we have monitored the structure of the surface by calculating the surface pair correlation function g(r) and the surface static structure factor s(k). We have also plotted out the averaged coordinates of the surface atoms so as to get a visual impression of the surface structure.

A). Main results of several trial potentials

We have performed the MD simulation for W(100) surface with several potentials under various conditions. Although not all the results are consistent with experimental results, they did provide some useful information for better understanding of the subject and guided us in choosing the optimal potential and simulation conditions. We would like to stress here some of main features from these calculations.

(1) One surface versus two surfaces

By using the bulk potential "BP-A" and the surface potential "sp-1" in the lattice hamiltonian (3.1), we have performed the MD simulation for the 8 layer slab with a) "sp-1" is imposed on two surfaces and b) "sp-1" imposed on top surface only, leaving the interaction for the bottom surface the same as bulk layer(one surface). The results show that in case a), although the reconstruction shows up in both surfaces (see Fig.4.1 for g(r)), the tow surfaces were found to interfere each other when the distortion of surfaces was established. In order to decouple the two surfaces, it is obvious that more thicker slab and thus more longer computer time is required. On the other hand, in the one surface simulation(case b), while the top surface gave C(2x2) structure, the bottom layer remained in undistored (1x1) structure. The surface pair corre-

lation functions for these two layers are shown in Fig 4.2 and Fig 4.3 respectively. Since the bottom layer in this case have a bulk structure, the interference of two surfaces was eliminated. With the same thickness of a slab we have more fraction of bulk layer compared to the case a) and the simulation is closer to the realistic situation.

(2) (T,V,N) ensemble versus (T,P,N) ensemble

We have performed the MD simulation for both (T,V,N) and (T,P,N) ensembles using the same potential "BP-A"+"sp-2"(on one surface). While the C(2x2) reconstruction was found in both ensembles, the larger lattice spacing in X-Y plane was found in the (T,P,N) ensemble(3.208A compared to 3.161A at T=100K). Since our MD cell is a very small fraction compared to the real system and in the simulation for the slab the periodic boundary condition is absent along the Z direction,the events on the surface may have strong influence on the bulk and probably change the bulk structure unrealistically if we let the MD cell free to change its volume and shape. In order to avoid this difficulty, it is convenient to use the (T,V,N) ensemble for our present surface investigation. Although the condition in (T,V,N) ensemble is not exactly the same as that in the experiment, the effect arising from the fixed MD cell seems smaller than that from unrealistic change of MD cell.

(3) Bulk potential "BP-B" versus "BP-A"

As have been discussed in the section III, the final choice of bulk potential "BP-B" have many advantages over the previous bulk potential "BP-A". We would like to present here further evidences by using them in the surface investigations. We performed the simulations by using the potential "BP-B"+"sp-2" and "BP-A"+"sp-2" for the same sample. The result turns out that with the potential "BP-A"+"sp-2" the surface atoms were found to "pop" up. We show in Fig.4.4 the corrspond surface pair correlation functions g(r) together with the vertical displacement of the surface atoms. When we start from low temperature T=100K,

we get a C(2x2) structure and only few atoms are "popped" up(Fig. 4.4(a)); while after heating to T=1000K then cooling to T=100K again, half of the surface atoms were found to "pop" up and the pair correlation function g(r) shown in Fig.4.4(b) is totally different from that in Fig.4.4(a). As a result this disordered structure turns to have lower energy. Conversely, by using the potential "BP-B"+"sp-2", this defect was found to be eliminated and the surface structure change was found to be revsable with temperature.

(4) Repulsive surface potential versus attractive surface potential

The surface potential "sp-1", which have a small attractive part, with mininum at r=3.83A as shown in Fig.3.1, has been used in our simulation. The results show that with this potential some surface atoms were found to fall into the minimum position of the potential.When we let the surface potential to be totally repulsive, as in the case of "sp-2", this defect was found to be eliminated. These features are shown in Fig.4.1 and Fig.4.4 respectively.

(5) 8x8 sample versus 4x4 sample

In order to study the size effect, we have performed a simulation on a 4x4 sample and a 8x8 sample with the same potential and under the same simulating conditions. The result turns out to be that qualitatively, both samples give almost the same features. However, the fluctuations in the 4x4 sample were found larger than in the 8x8 sample. The structure factor and surface energy have been compared for both samples in Fig.4.11 and 4.9, using the potential "BP-B"+"sp-3" as shown in Fig.3.2. It is obvious that for the quantitative analysis, we have to use the 8x8 sample. Probably larger samples are needed to check the adequacy of an 8x8 sample.

To sum up, we have performed the MD simulation with several trial po-

tentials under various conditions. The results led us to conclude: a) bulk potential "BP-B" is better than "BP-A"; b)the best surface potential is one which is totally repulsive; c) the surface potential imposed on one surface is better than imposed on two surfaces; d) (T.V.N) ensemble is more convenient than (T.P.N) ensemble for our surface investigations; e) for the quantitative analysis, we should adopt the 8x8 sample for the moment.

B). The results of "BP-B"+"sp-3"

The final choice of potential "BP-B"+sp-3"(impose on top surface) has been investigated in detail for 8x8 sample. The simulations were performed at constant temperature (T.V.N) ensemble, for various temperatures T=50,100, 150, 200, 300, 400, 500K. The main results are sumarized in table 1 In Fig. 4.5 and Fig.4.6, we have plotted out the average surface atom coordinates respect to the ideal squre lattice at T=50K and T=400K respectively. The pictures show well the periodic distortion of the surface atoms from the ideal square lattice to form the C(2x2) superlattice at low temperature, while at high temperature the surface atoms were found to form a 1x1 structure, apart from some small deviations. The surface structure factors at various K point as listed in table 2 also show that an extra peak shows up at k= $(\frac{1}{2},-\frac{1}{2})\frac{2\pi}{a}$ at low temperature and disappears gradually when the temperature is increased. The calculated surface pair correlation functions as shown in Fig.4.7 are also compatible with Fig.4.5 and Fig.4.6, thus further confirming the existence of the C(2x2) reconstruction of W(001) surface. We also looked at the distortion amplitude decaying into the bulk and the result showed the exponentially decaying behaviour as in Fig. 4.14.

In order to study the temperature dependent phase transition of W(100) surface, we have evaluated the energies and the distortion amplitudes for various temperatures. The behaviour of the total energy E and the surface

energy Es with temperature T are drawn in Fig.4.8 and Fig.4.9(together with the 4x4 sample results). The interlayer surface energy E's difined by (2.23) is shown in Fig.4.10. The Fig.4.11 and Fig.4.12 show the surface structure factor s(k) for $k=(\frac{1}{2}, -\frac{1}{2})\frac{2\pi}{a}$ and the order parameter d (the average displacement amplitude of the surface atoms along the (1,-1) direction with respect to the squre lattice) for various temperature T. The results show the gradual decrease of order parameter with the increase of the temperature. Finally, the specific heat calculated by means of the energy flactuation as described in Sec II is plotted in Fig.4.13. More discussion about these results will give in the following section.

TABLE 1. THE RESULTS OF "BP-B"+"SP-3" FOR A 8x8 SAMPLE.

T(k)	E (ev)	Es (ev)	E's (ev)	C_v^b (Kb)	C_v^s (Kb)	Z(A)	d(A)	$S(K)_3$ X10
50	-6.96459±.00030	.44421±.0028	1.77183±.0023	2.68	-.53	.0085	.1449	40.8
100	-6.95218±.00066	.45114±.0025	1.77631±.0020	3.02	0.22	.0132	.1157	26.3
150	-6.93984±.00099	.45978±.0037	1.78238±.0030	3.02	1.61	.0148	.0731	10.5
200	-6.92759±.00130	.46646±.0042	1.78720±.0035	2.95	1.54	.0189	.0613	7.4
250	-6.91554±.00163	.47282±.0045	1.79209±.0040	2.96	1.40	.0219	.0537	6.1
300	-6.90365±.00200	.47771±.0050	1.79615±.0044	3.09	1.55	.0242	.0423	4.1
400	-6.87998±.00263	.48419±.0066	1.80143±.0060	2.99	1.31	.0286	.0271	2.3
500	-6.85642±.00315	.49218±.0081	1.80851±.0073	2.75	1.90	.0336	-.0137	0.7

V. DISCUSSIONS

Although there is still some controversy on the precise atomic structure of the low temperature phase of W(100) surface experimentally, our present MD results is based onto Debe-King model. We conclude that the C(2x2) structure as in Fig.4.5 to be the most stable structure of W(100) surface at low temperature on the following ground: (a) Starting from an ideal (1x1) square lattice, the surface atoms were found to distort spontaneously along the (1,-1) direction and finally reach the equilibrium configuration of Fig.4.5. In order to make sure the system is in equilibrium, we have performed two consecutive averaging "job", each of 2000 MD steps, at same temperature and compared the results which turned out to be the same; (b) We have heated the system from T=100K to T=300K then cooled it to T=100K again. It was found that the configuration of surface atoms before and after heating--cooling procedure were the same at T=100K. Thus the structure change seems reversible with temperature T.

The high temperature structure of W(100) surface, on the other hand,was found in our MD simulation to be disorder 1x1 structure as shown in Fig.4.6, which is consistent with the experimental observations.

The periodic lattice distortion is generaly accompaned by soft modes. Our result of MD simulation further supports the FST's lattice dynamics model, which is based on the soft mode approach. With several set of surface force constants α_s, β_s chosen from the M_5 region of phase diagram Fig.2 , our MD simulation has shown the C(2x2) reconstruction on the W(100) surface at low temperature. It seems that the lattice Hamiltonian(3.1) is plausible for the description of the reconstruction of W(100) surface even it is still limited to the classical scheme.With the potential "BP-B"+"sp-3" in the Hamiltonian (3.1), most properties of the reconstruction of W(100) surface have been

reproduced. Fig.5.1 compares our MD results of surface structure factor s(K) ($K=\frac{2\pi}{a}(\frac{1}{2},-\frac{1}{2})$) to that of LEED experiment result of King and Thomos. It turns out that our MD result is very similar to that of experiment, though the trnsition temperature still seems to be lower in our case. We believe that based on the phase diagram Fig. 2, we can finally obtain a set of optimal surface parameters for the lattice Hamiltonian (3.1) which can reproduce well the experimental results.

Surface reconstructions are phase changes affecting only a few layers of a 3D crystal and their behaviour should be entirely 2D. However, the critical behaviour of surface reconstruction is still unclear either experimentally or theoretically, except that the W(100) transitions seem continuous. In our work of MD simulation., we have spent a lot of effort for the understanding of phase transition on W(100). We would like to present here some discussions on our present results though the problem is not yet finally solved.

The result of our MD simulation seems to suggest the second-order structural phase transition for the W(100) surface reconstruction. By looking at Fig.4.5 and Fig.4.6, it is easy to identify the point group of the low temperature phase as C_{2v}, while that of the high temperature phase as C_{4v}. Obviously C_{2v} is a subgroup of C_{4v}. The order parameter describing the reconstruction of W(100) surface as in Fig. 4.5 is the surface atom distortion. It has been pointed out by Tosatti[6,14] that the representation of this order parameter is M_5 characterized by K= M(1/2,1/2)2π/a. Our result of surface structure factors do show an extra peak at K=(1/2,-1/2)2π/a. All these evidences are consistent with the conditions required by Landau theory of second order phase transition.

However, for a second order phase transition, it is generally expected that the specific heat of the system should show the discontinuty at transition temperature T_c(or equivelently the E~T curve should change the

slope at T_c). As we look at the E~T curve in Fig. 4.8, it is hard to find out the change of slope. The calculated total specific heat C_v^b as shown in Fig. 4.13 is almost constant. It was realized that in the calculated total energy and total specific heat, the contribution from the bulk atoms dominate that from the surface atoms. Since the surface reconstruction is the structure change mainly on the surface layer, while the structure of the bulk remain unchanged, it is not easy to find out the changing slope of the total energy during the transition.

In order to overcome this difficulty, we have tried to extract the part of contribution to the energy and the specific heat coming from the surface atoms. For this purpose, the surface energy E_s defined as (2.22) and the surface interlayer energy E_s' defined as (2.23) have been evaluated (see Fig. 4.9 and Fig. 4.10). These two quantities were found to have similar temperature behaviour and seems do change the slope at T~250 K. If we identify this temperature as the transition temperature T_c, it seems to be little too high compared to the behaviour of the order parameter and the structure factor(see Fig.4.11 and Fig. 4.12). However, the surface specific heat C_V^s calculated through (2.30) and shown in Fig. 4.13 seems no discontinuty to be found around T = 200K or 250K. We have also tried to evaluate other quantities associated to the surface energy flactuation. These quantities are $Q_1 = \langle (\Delta E_s)^2 \rangle / k_B T^2$ and $Q_2 = \langle (\Delta E_s')^2 \rangle / k_B T^2$. The benaviour of Q_1 and Q_2 with the temperature is plotted in Fig. 5.2, which do show the discontinue around T=200K. Unfortunely, the magnitude of Q_1 and Q_2 were found to be large than the slope of the E_s~T and E_s'~T curve approximately by a factor of 3. Thus the meaning of these quantities is yet unclear. For the moment we still can not arrive at the conclusion on the nature of the transion of the W(100) surface and we leave this problem for further investigations.

In conclusion, with our MD method we have obtained a bulk potential of W which gives stable B.C.C. structure of bulk W and has a good thermal expansion behaviour compared to the experiment at least at low temperature (0~T~2500K). For the W(100) clean surface, we have obtained a C(2x2) structure at low temperature and a (1x1) structure at high temperature, which is compatible with the experiment and existing models though the transition temperature still seems too low . Many evidences from our simulation results tend to suggest that the W(100) surface reconstruction is second order structural phase transition. However, the nature of this transition is yet unclear and we leave it for further investigation. With the effective lattice Hamiltonian, we have shown that the MD method is an useful tool in the study of surface reconstruction. The application of the method for the investigation of other similar systems such as Mo(100) surface, we hope, will be straightforward. The method can also be applied without much difficulty to the chemisorption system, such as H/W(100), where we shall have to take account of the adatom-adatom and adatom-substrate interactions in some suitable manner. We hope this will be our future work.

ACKNOWLEDGEMENT

This work has been carried out under the supervision of Prof. E. Tosatti and Prof. M. Parrinello. The author wishes to thank them for their kind guidance and encouragement throughout the couse of this study. Most work presented in Chapter III concerning optimal potential to describe W(100) has been done in collaborate with A. Fasolino and A. Franchini. The author thank them for many useful discussions during the work, and specially A. Franchini for her generous help at the early stages of this work. He also wishes to thank Dr. T. Takemori and A. Fasolino for many valuable suggestions and critical reading of the manuscript.

REFERENCES

(1) T.E.Falter, R.A.Barker and P.J.Estrup, Phys. Rev. Letters 38, (1977) 1138

(2) P.J.Estrup, F.Jona and P.M.Marcus, Solid State Commun. 25, (1978) 375

(3) M.K.Debe and D.A.King, J.Phys.C10, (1977) L303;Phys. Rev. Letters 39, (1977) 708

(4) M.K.Debe and D.A.King, Surf.Sci. 81, (1979) 193;D.A.King and G.Thomas, Surf. Sci. 92, (1980) 201 and references therein

(5) T.T.Tsong and J.Seeney, Solid State Commun. 30, (1979) 767

(6) E.Tosatti, Solid State Commun. 25, (1978) 881

(7) E.Tosatti and P.W.Anderson, Solid State Commun. 14, (1974)773

(8) J.E.Inglesfield, J.Phys. C11, (1978) L69

(9) K.Terakura, I.Terakura and Y.Terakura, Surf. Sci. 86, (1979)535

K.Terakura, I.Terakura and N.Hamada, Surf. Sci. 103, (1981) 103

(10) H.Krakauer,M.Posternak and A.J.Freeman, Phys.Rev. Letters 43, (1979) 1885

(11) P.C.Stephenson and D.W.Bullett,in: Europhysics Conf.Abstracts, 1982, Vol.6A, Ed. V.Heine (European Physical Society, 1982); Surf. Sci. 139, (1984) 1

(12) J.C.Campuzano, D.A.King, C.Somerton and J.E.Inglesfield, Phys. Rev. Letters 45, (1980) 1649

(13) S.C.Ying and L.D.Roelofs, Surf.Sci.125, (1983) 218

(14) E.Tosatti, in:Karpacz Winter School of Theoretical Physics, Ed. A.Pekalski and J.Pryzstawa(Springer,Berlin,1979)

(15) A.Fasolino, G.Santoro and E.Tosatti, Phys.Rev.Letters 44, (1980) 1684

(16) A.Fasolino, G.Santoro and E.Tosatti, Surf.Sci. 125, (1983) 317

(17) L.D.Roelof, G.Y.Hu and S.C.Ying, Phys.Rev. B28, (1983) 6369

(18) C.Y.Hu and S.C.Ying, to be published

(19) G.Y.Hu, L.D.Roelof and S.C.Ying, to be published

S.C.Ying in: Erice Summer School on "Dynamical Phenomena at Surfaces, Inter-

faces and Superlattices", July 1984)

(20) M.Parrinello and A.Rahman, Phys. Rev. Letters. 45, (1980) 1196

(21) M.Parrinello and A.Rahman, J.Appl. Phys. 52, (1981) 7182

(22) M.Parrinello, A.Rahman and P.Vashishta, Phys. Rev. Letters 50, (1983) 1073

(23) S.Nose and M.L.Klein, J. Chem. Phys. 78, (1983) 6928

(24) S.Nose and M.L.Klein, Phys. Rev. Letters 50, (1983) 1207

(25) S.Nose and M.L.Klein, Molec. Phys. 50, (1983) 1055

(26) H.C.Andersen, J.Chem. Phys. 72, (1980) 2384

(27) L.V.Woodcock, Chem. Phys. Lett. 10 (1971) 257

(28) F.F.Abraham, S.W.Koch and R.C.Desai, Phys. Rev. Letters 48, (1982) 1818

(29) R.H.Friend and D.Jerome, J.Phys. C12, (1979) 1441

(30) For a review on quasi-1D CDWs see G.A.Toombs, Phys. Repts. 4oc, (1978) 182

(31) M.J.Rice and S.Strassler, Solid State Commun. 13, (1973) 125

(32) D.Castiel, L.Dobrzynski and D.Spanjaard, Surf. Sci. 59, (1976) 252

(33) S.Nose, Molec. Phys. 52, (1984) 255

TABLE 2. THE SURFACE STRUCTURE FACTOR

T = 400 K

Kx ($\frac{2\pi}{a}$) \ Ky ($\frac{2\pi}{a}$)	-1	-3/4	-1/2	-1/4	0
1	36014.98	45.72	30.97	29.18	38429.63
3/4	48.55	56.73	46.84	40.59	24.97
1/2	51.83	29.07	93.53	10.42	4.49
1/4	33.83	31.17	9.62	6.04	3.00
0	38621.06	11.59	8.22	1.20	40960.00
-1/4	39.66	18.38	22.38	6.40	3.00
-1/2	35.07	24.23	9.14	8.41	4.49
-3/4	68.61	59.21	86.61	32.37	24.97
-1	36437.09	31.19	31.62	30.62	38429.63

T= 50 K

Kx ($\frac{2\pi}{a}$) \ Ky ($\frac{2\pi}{a}$)	-1	-3/4	-1/2	-1/4	0
1	34068.04	4.59	2.09	4.35	38976.07
3/4	4.39	6.61	5.64	3.59	1.72
1/2	3.74	1.98	1672.49	1.07	1.12
1/4	4.77	4.77	.93	.59	.14
0	38929.25	2.39	.47	.21	40960.00
-1/4	5.65	6.04	1.50	.72	.14
-1/2	5.62	6.99	1.13	2.54	1.12
-3/4	6.73	6.07	7.30	4.80	1.72
-1	40133.16	6.41	1.74	5.00	38976.07

&& All numbers listed in the table have been amplified by a factor of 40960.

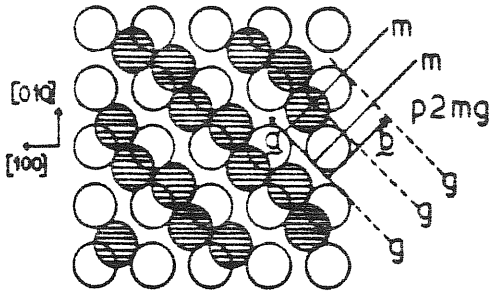

FIG. 1. A top-layer rearrangement ball model for a $(\sqrt{2} \times \sqrt{2})R45^0$ domain having $p2mg$ symmetry. For a single-layer rearrangement model, this structure appears to be unique. The primitive unit mesh is defined by $\vec{a}$ and $\vec{b}$ and its symmetry elements are indicated: g = glide plane, m = mirror plane.

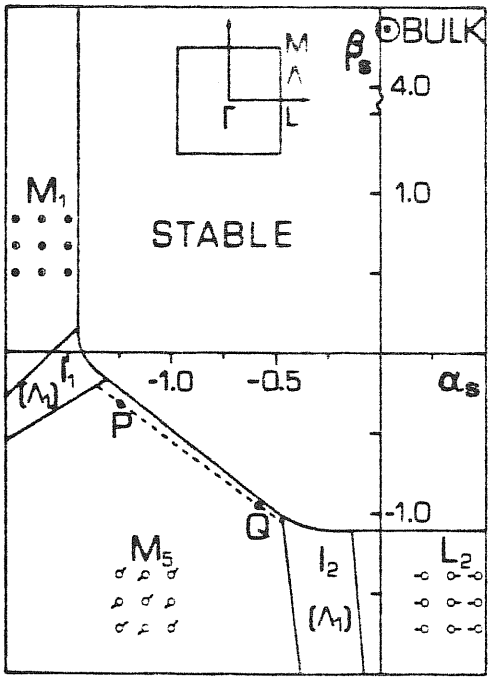

FIG. 2. $T = 0$ phase diagram as a function of surface forces α_s and β_s, in units of THz^2 g for W(100). The regions M_1, M_5, and L_2 are commensurate (first-layer distortions are sketched), while I_1 and I_2 are incommensurate, with a Λ_1-type distortion. The clean W(100)$(\sqrt{2}\times\sqrt{2})45^\circ$ surface is described by a point on the P–Q line.

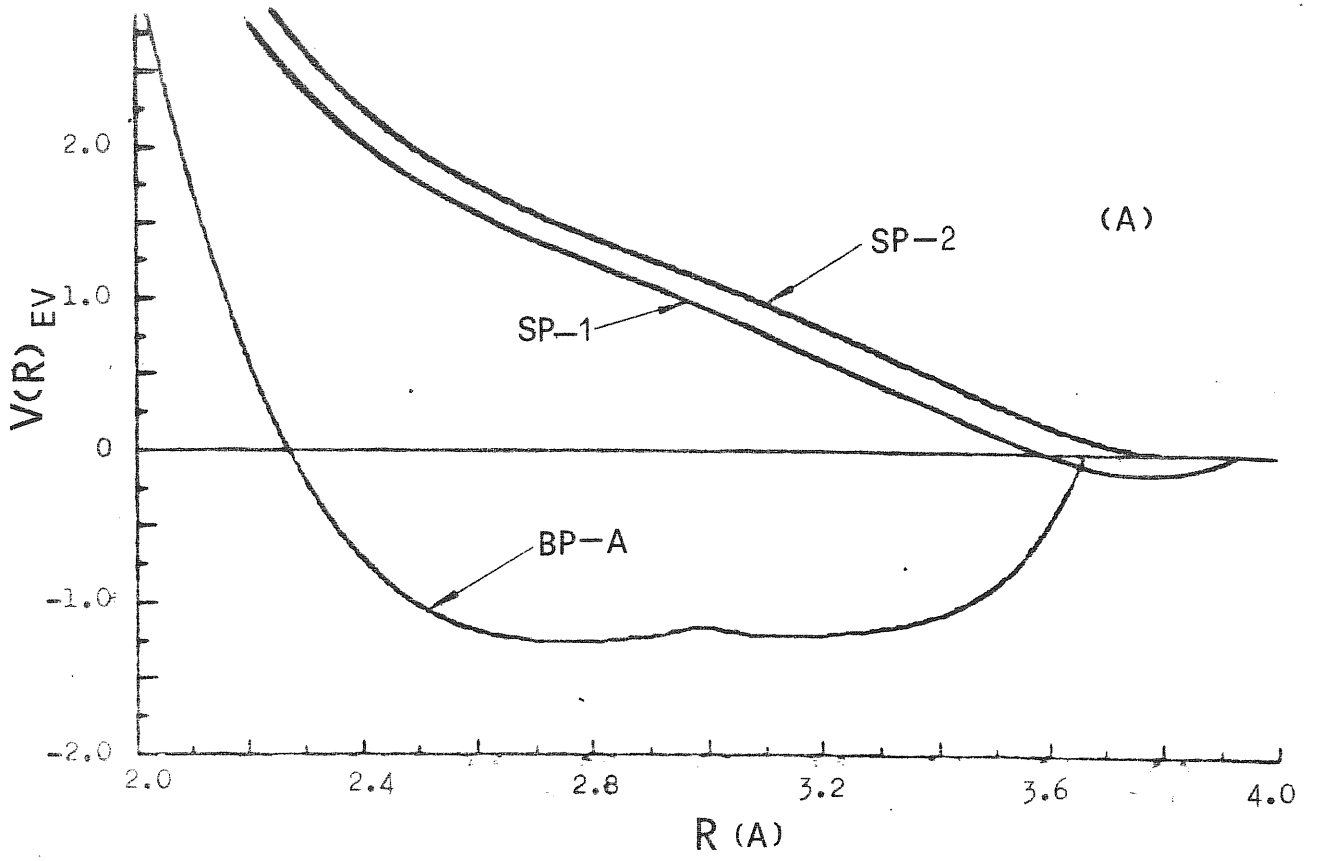

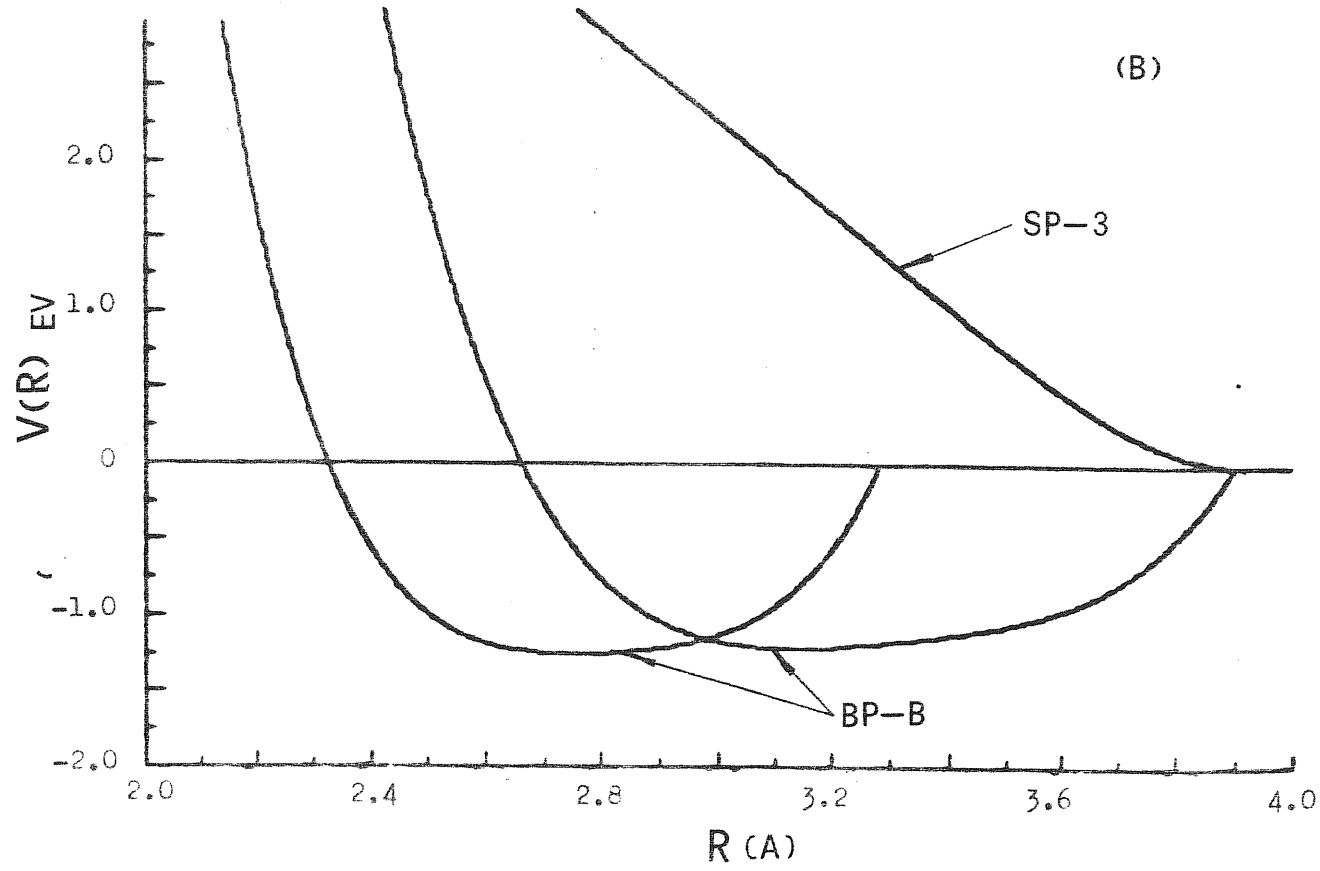

Fig. 3.1 The potentials

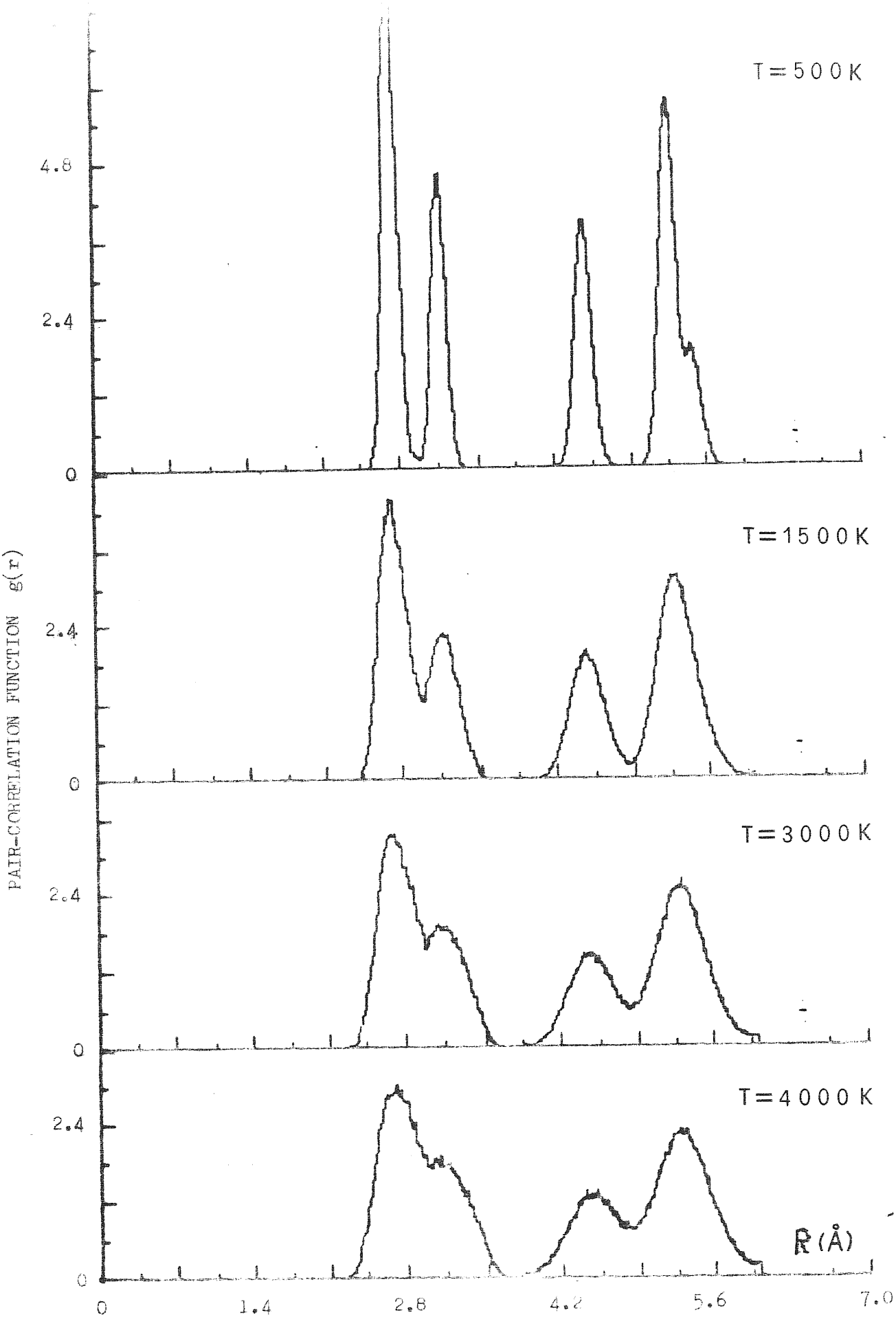

Fig. 3.2 The pair correlation function g(r) of bulk W by using the potential "BP-A".

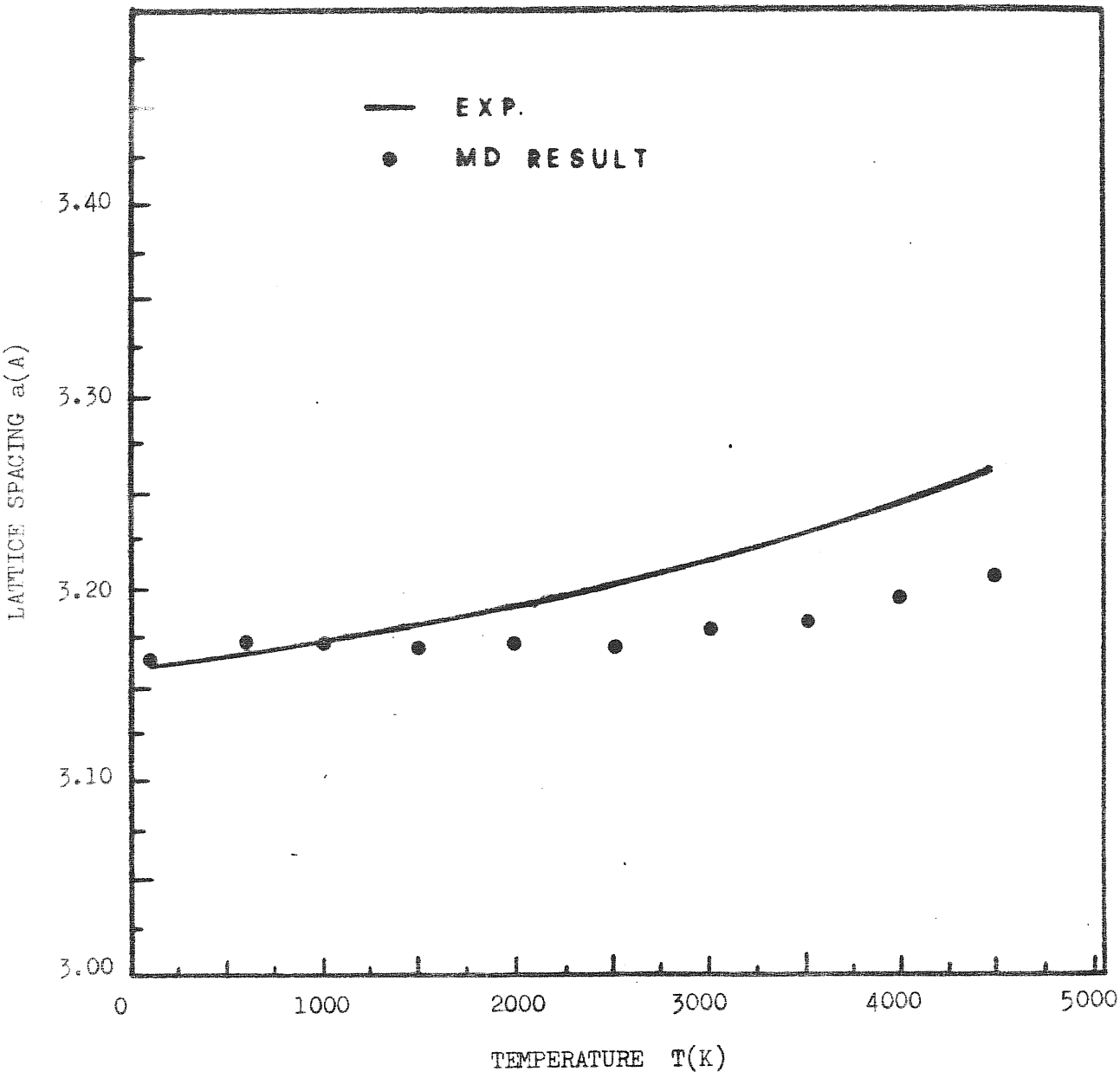

Fig. 3.3 The thermal expansion of bulk W by using the potential "BP-A".

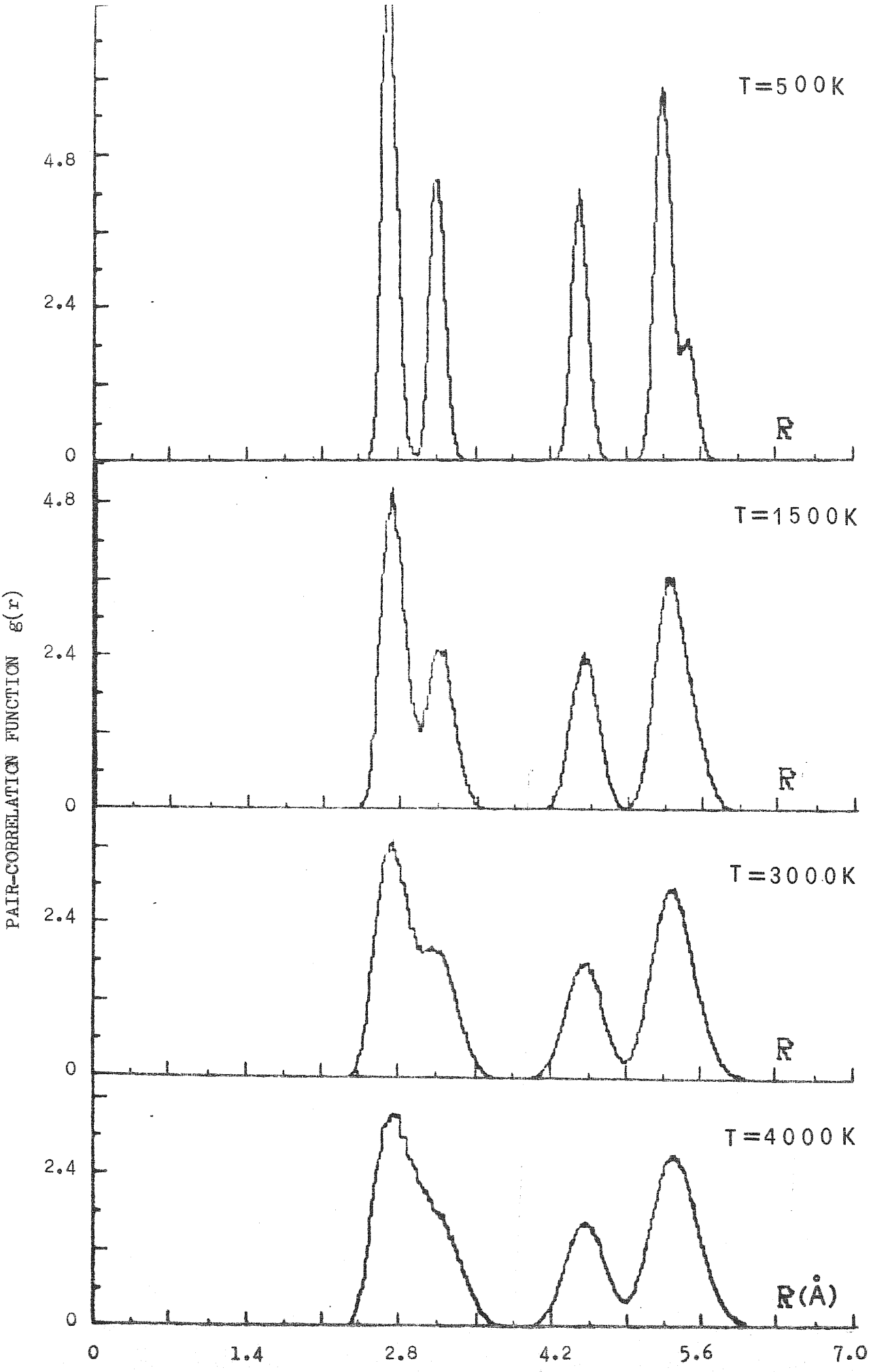

Fig. 3.4 The pair correlation function g(r) of bulk W by using the potential "BP-B".

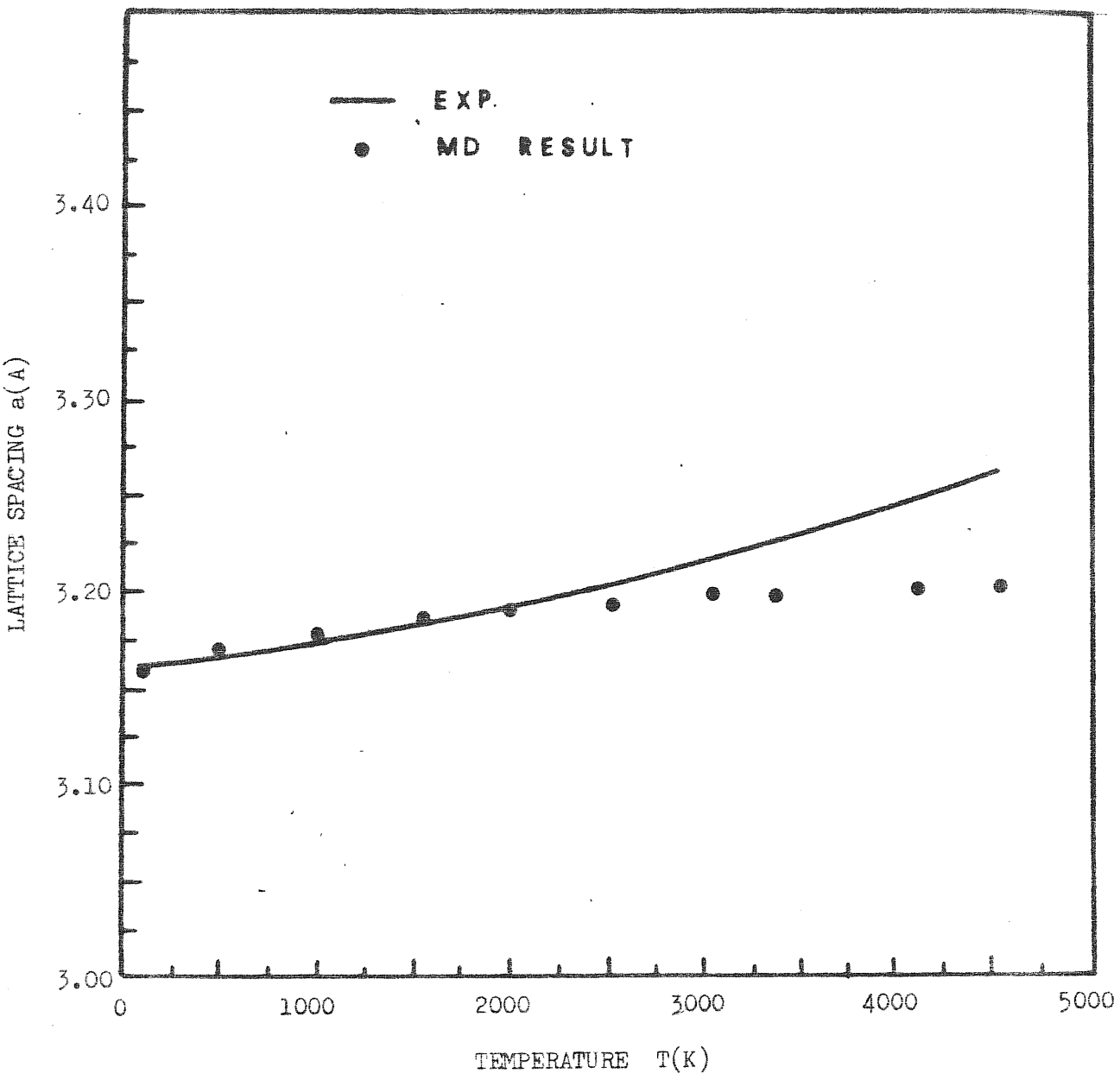

Fig. 3.5 The thermal expansion of bulk W by using the potential "BP-B".

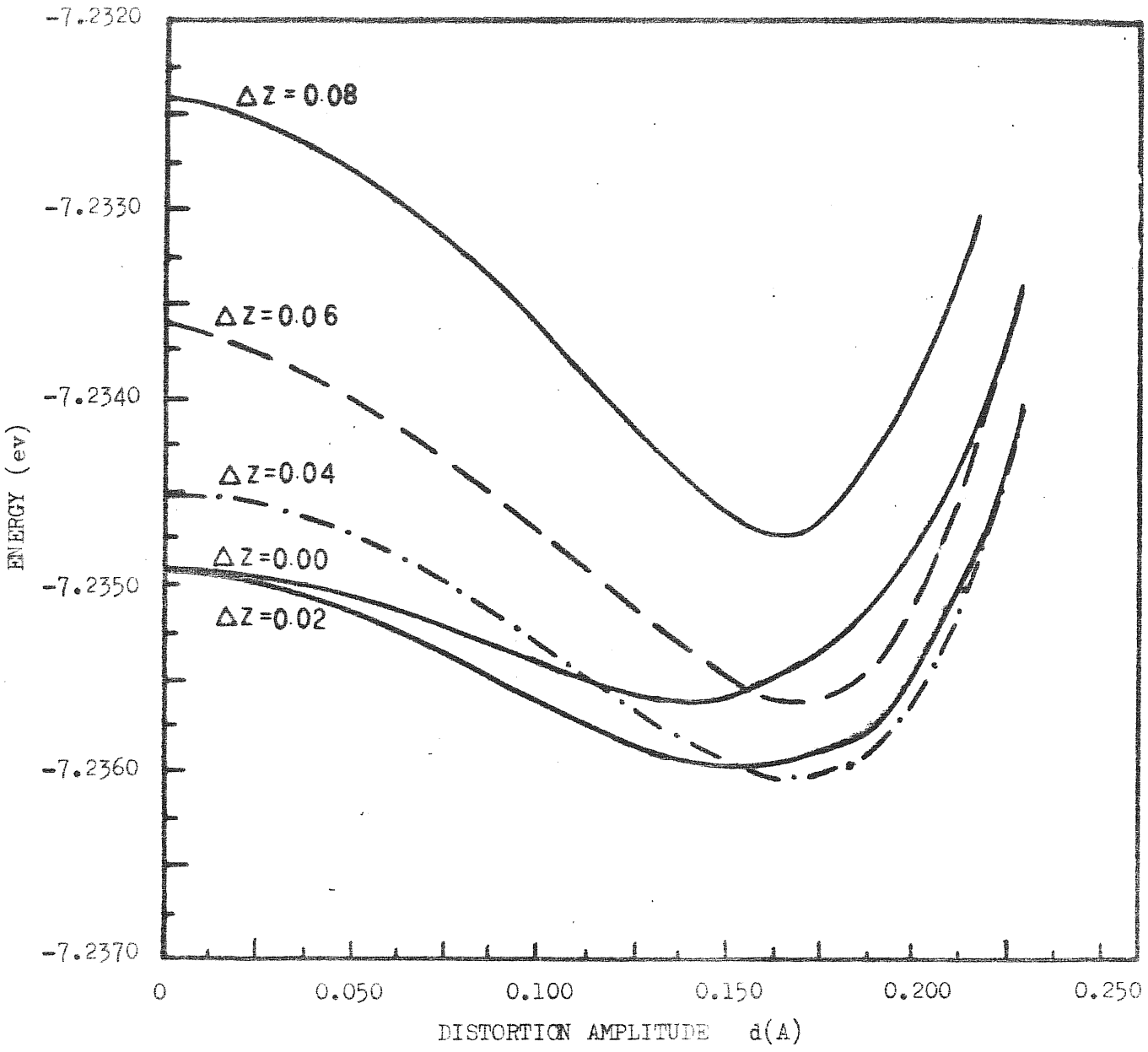

Fig. 3.6 The configuration energy (T=0K) of a 8-layer slab W with a C(2×2) (100) surface for various distortion amplitude d by using the potential "BP-A"+"SP-1". ΔZ denotes the vertical relazation of the surface layer.

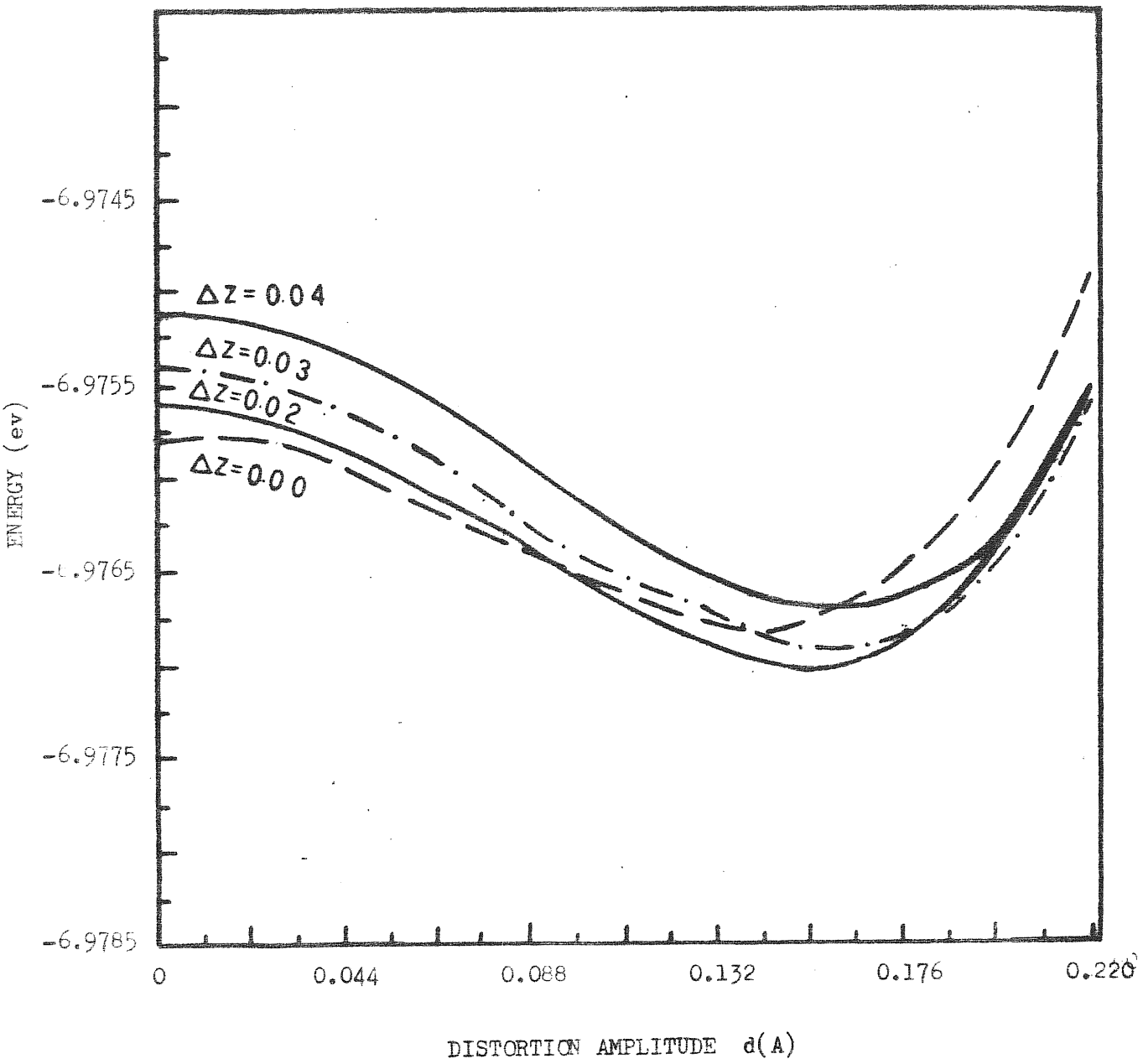

Fig. 3.7 The configuration energy (T=0K) of a 8-layer slab W with a C(2x2) (100) surface for various distortion amplitude d by using the potential "BP-B"+"SP-3". ΔZ denotes the vertical relazation of the surface layer.

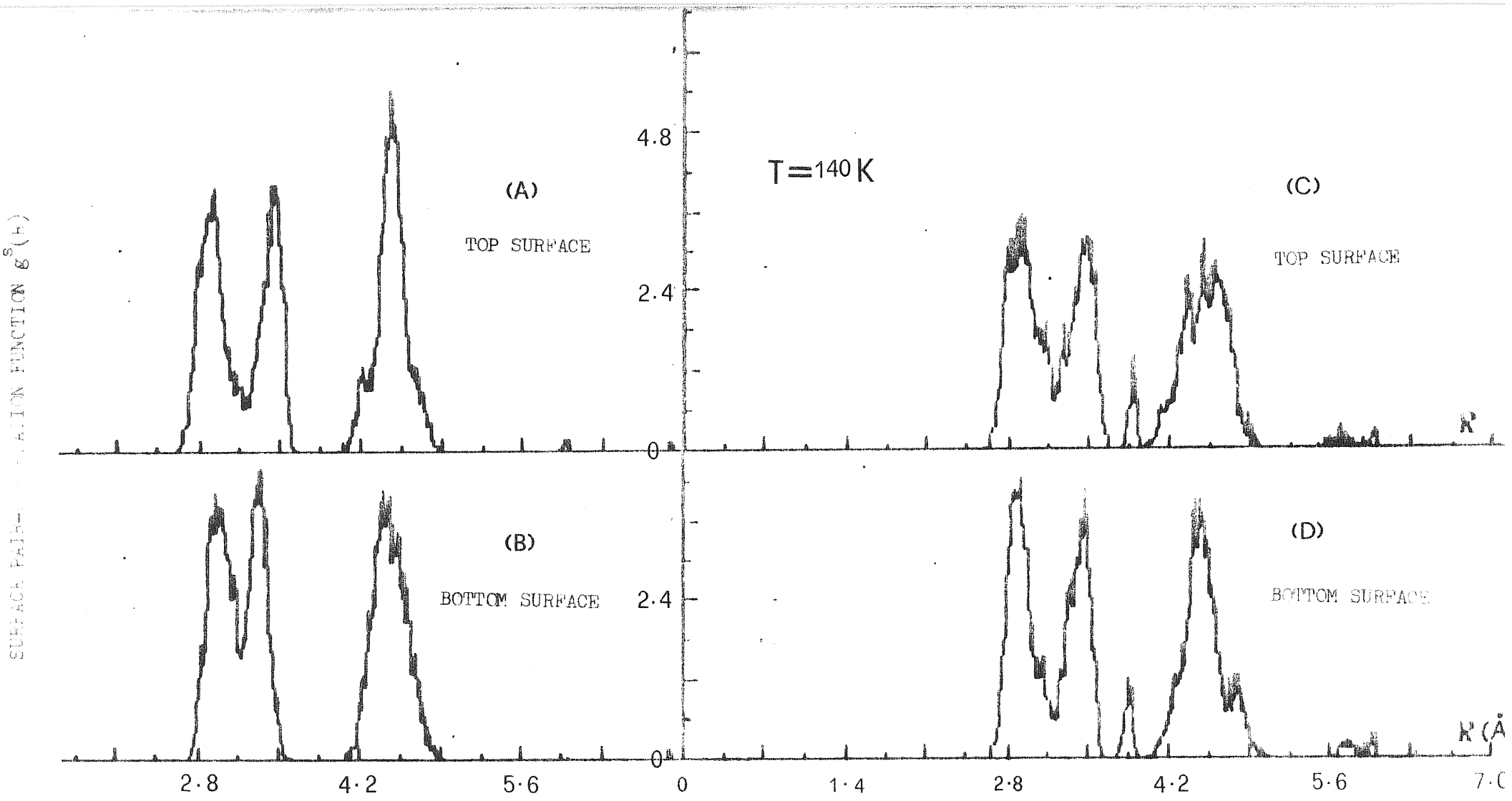

Fig. 4.1 The surface pair correlation function $g^S(R)$ for both top and bottom W(100) surfaces at T = 140K, using the potential "BP-A"+"SP-1"(imposed on two surfaces).

(a) and (b) are the results obtained by starting from the low temperature.

(c) and (d) are the results obtained by cooling from T = 200 K.

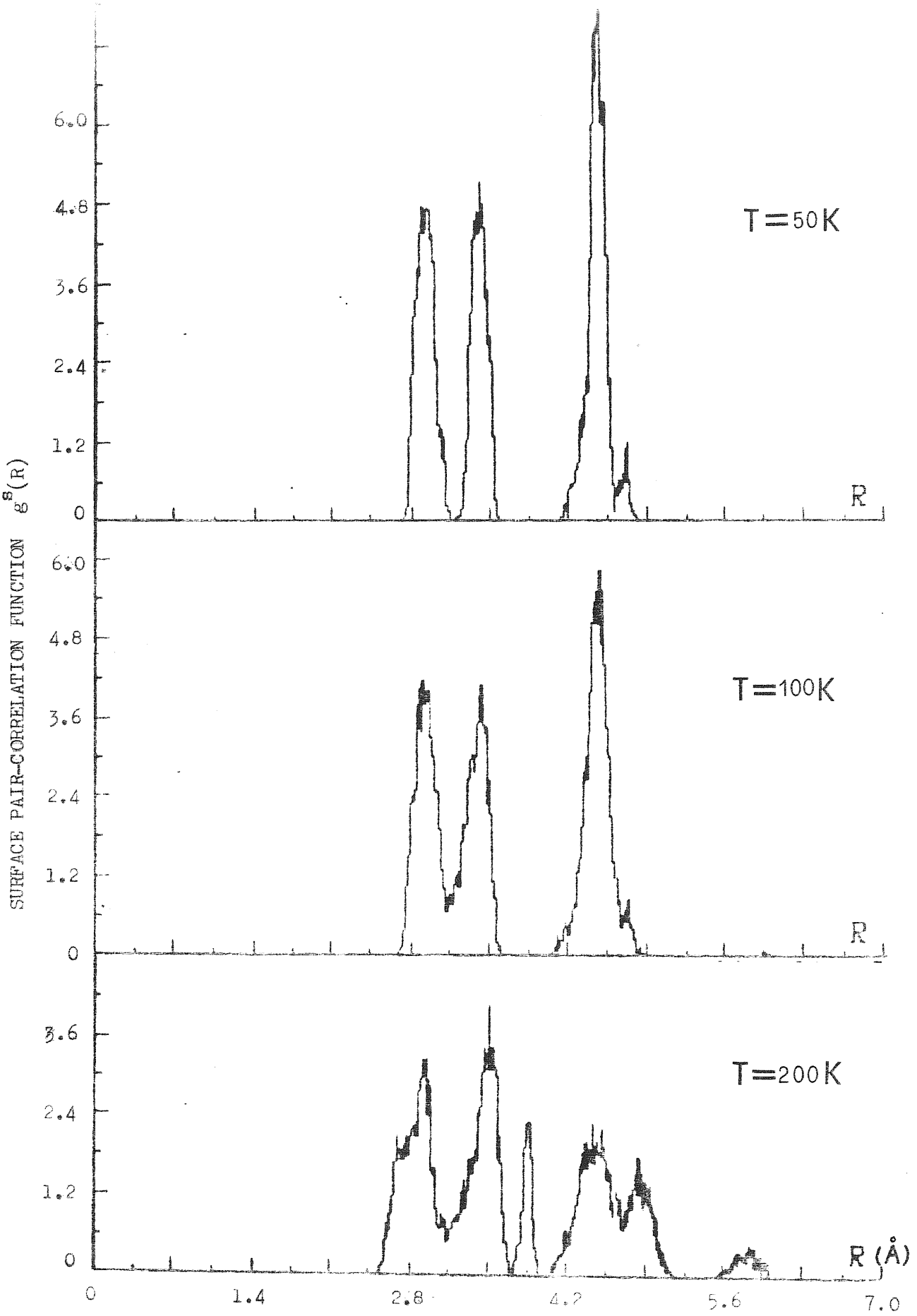

Fig. 4.2 The surface pair correlation function $g^s(R)$ of the top surface, using the potential "RP-A"+"SP-1"(SP-1 was imposed on top surface).

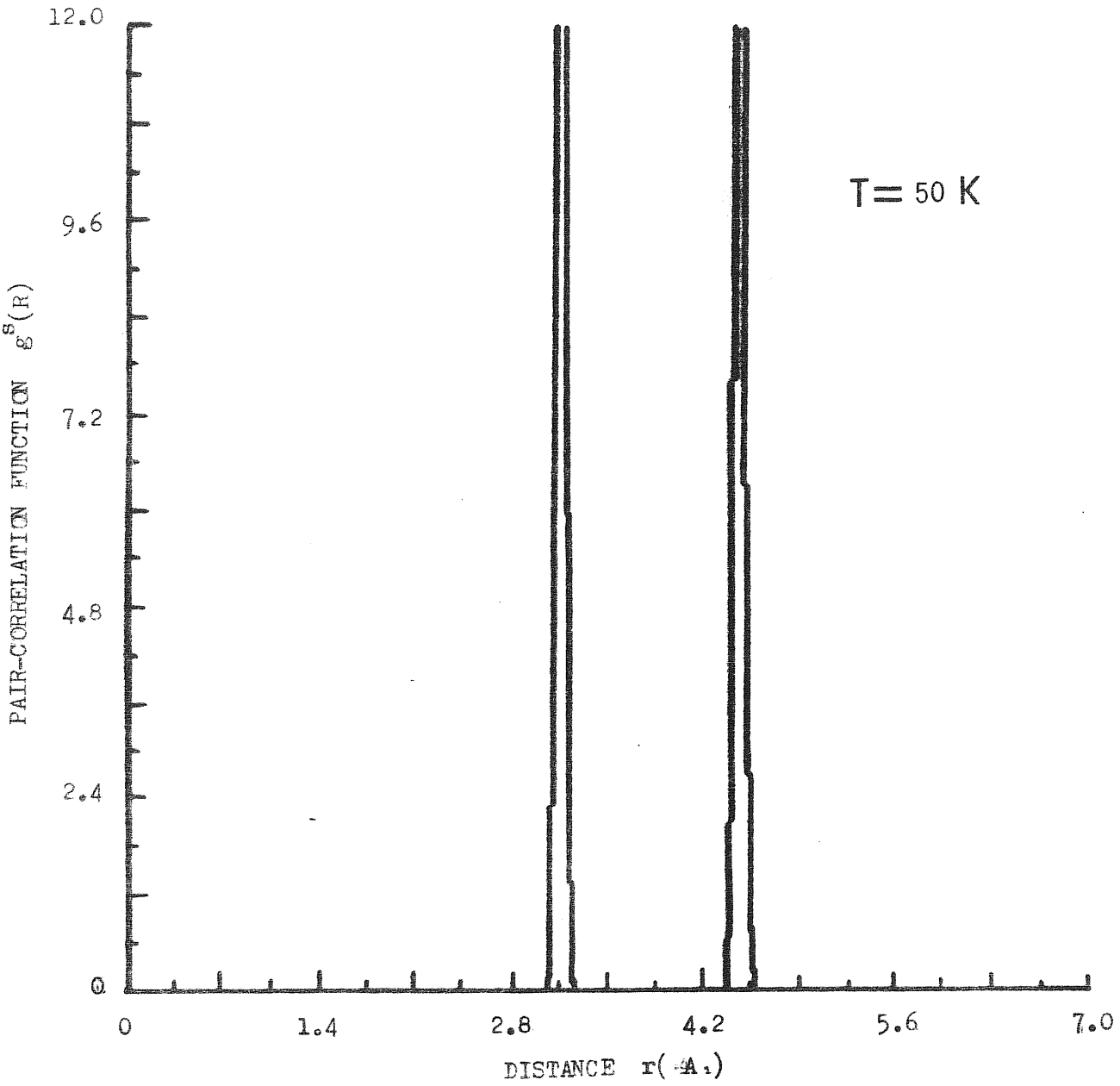

Fig. 4.3 The surface pair correlation function $g^s(R)$ of the bottom surface, using the same potential as that for Fig. 4.2.

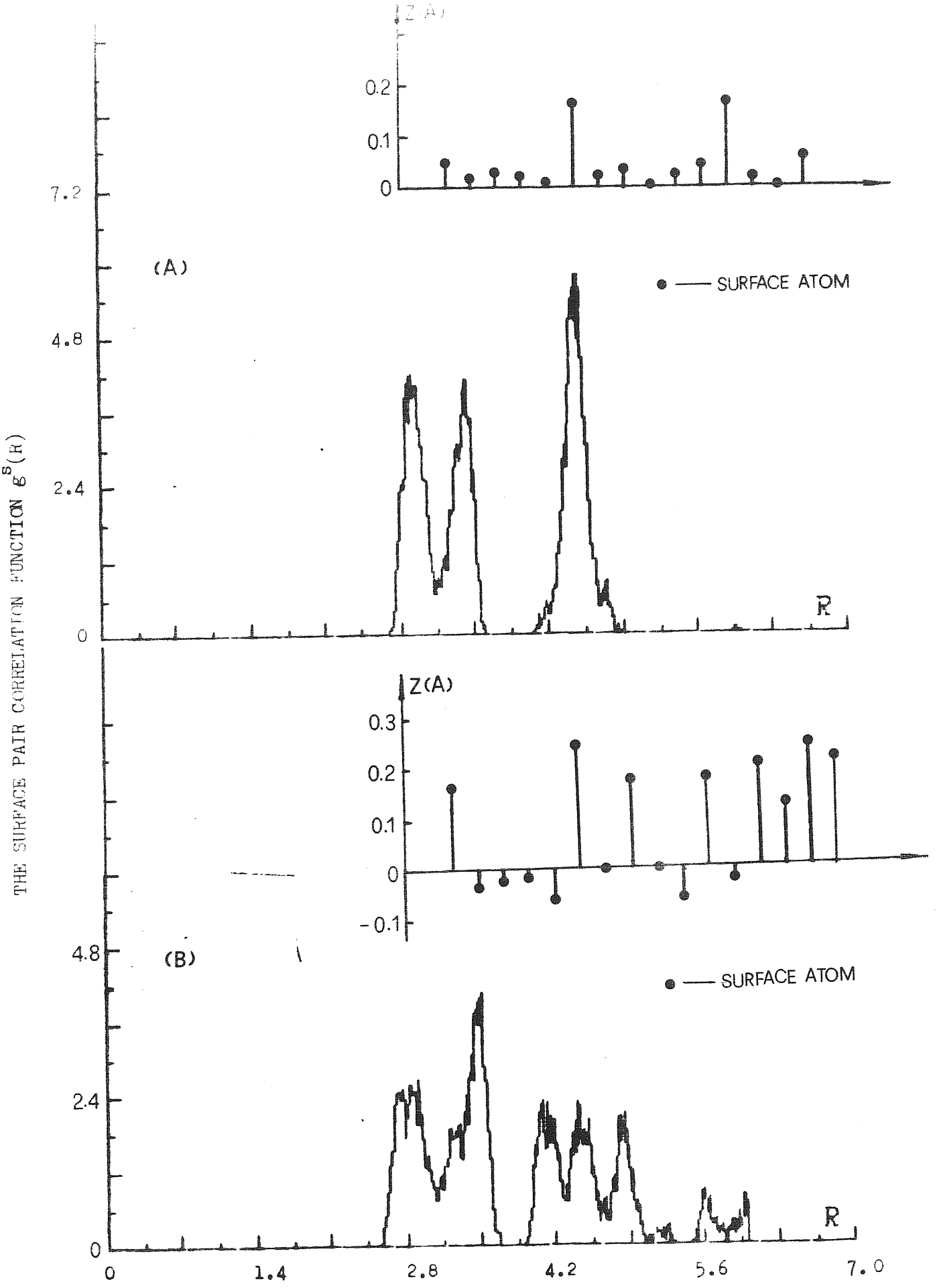

Fig. 4.4 The surface pair correlation function $g^S(R)$ of the top surface using the potential "BP-A"+"BP-2"(imposed on top surface), together with the correspond.averaged Z-component of the surface atoms for the following case (a), start from the low temperature T = 100 K. (b), heat the system from the configuration of (a) to T = 1000 K, then cool it to T = 100 K.

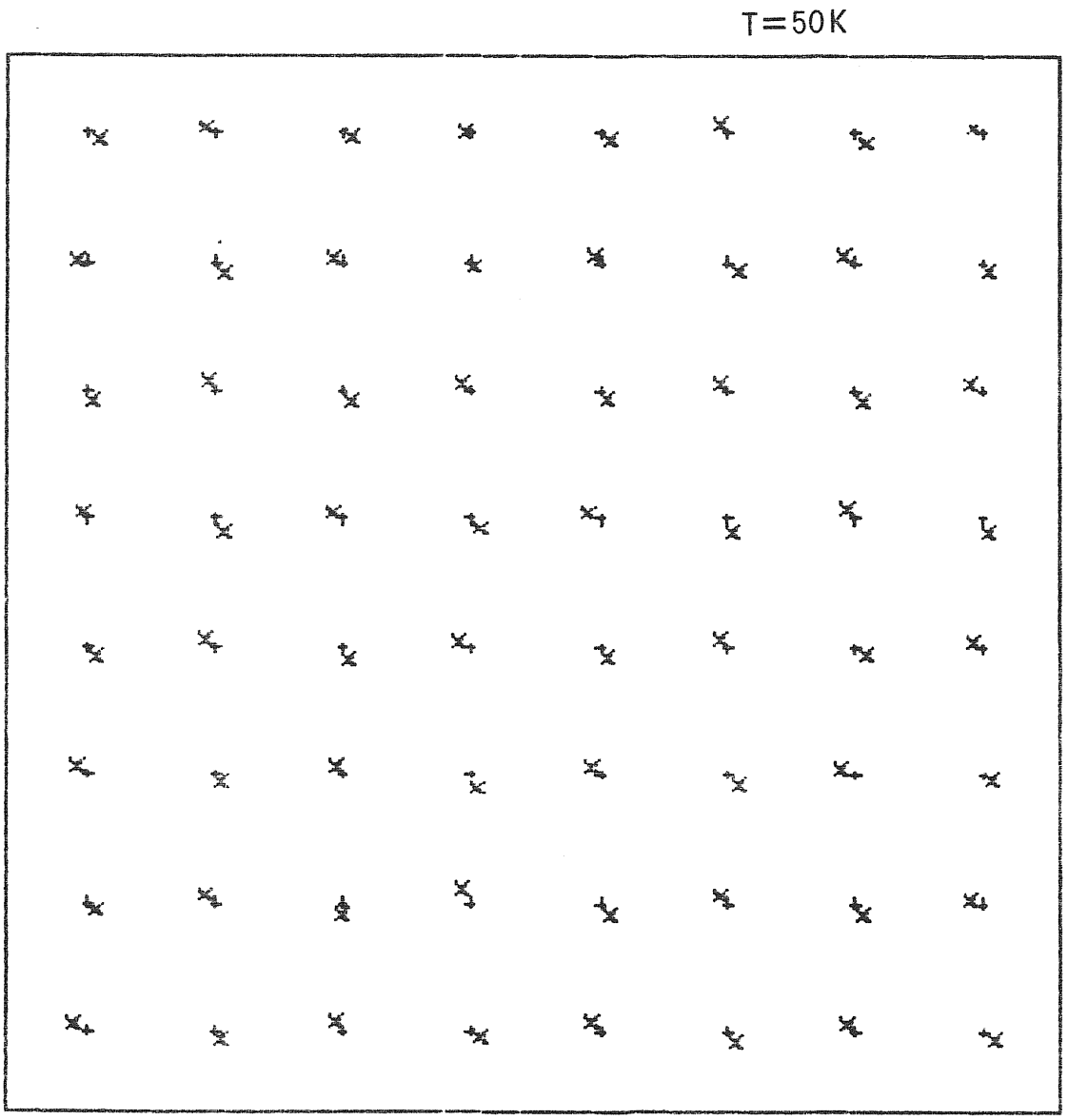

Fig. 4.5 The plot of averaged coordinates of the surface atoms at T = 50 K using the potential "BP-B"+"SP-3" for a 8x8 sample.

"+" refer to the 1x1 square lattice site.

"x" refer to the averaged surface atom coordinates in X-Y plane.

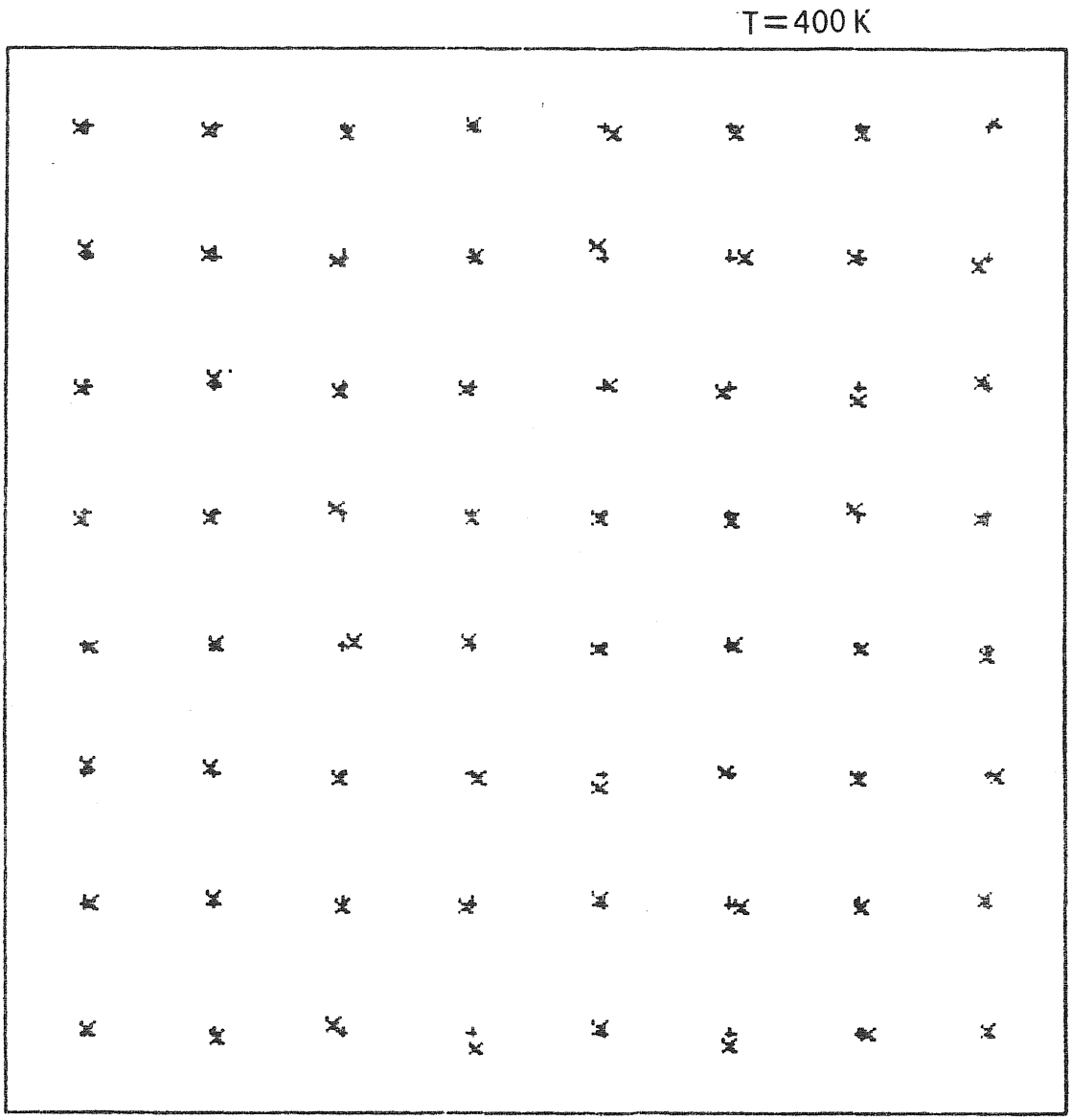

Fig. 4.6 The plot of averaged coordinates of the surface atoms at T= 400 K using the potential "BP-B"+SP-3" for a 8x8 sample.

"+" refer to the 1x1 square lattice site.

"x" refer to the averaged surface atom coordinates in X-Y plane.

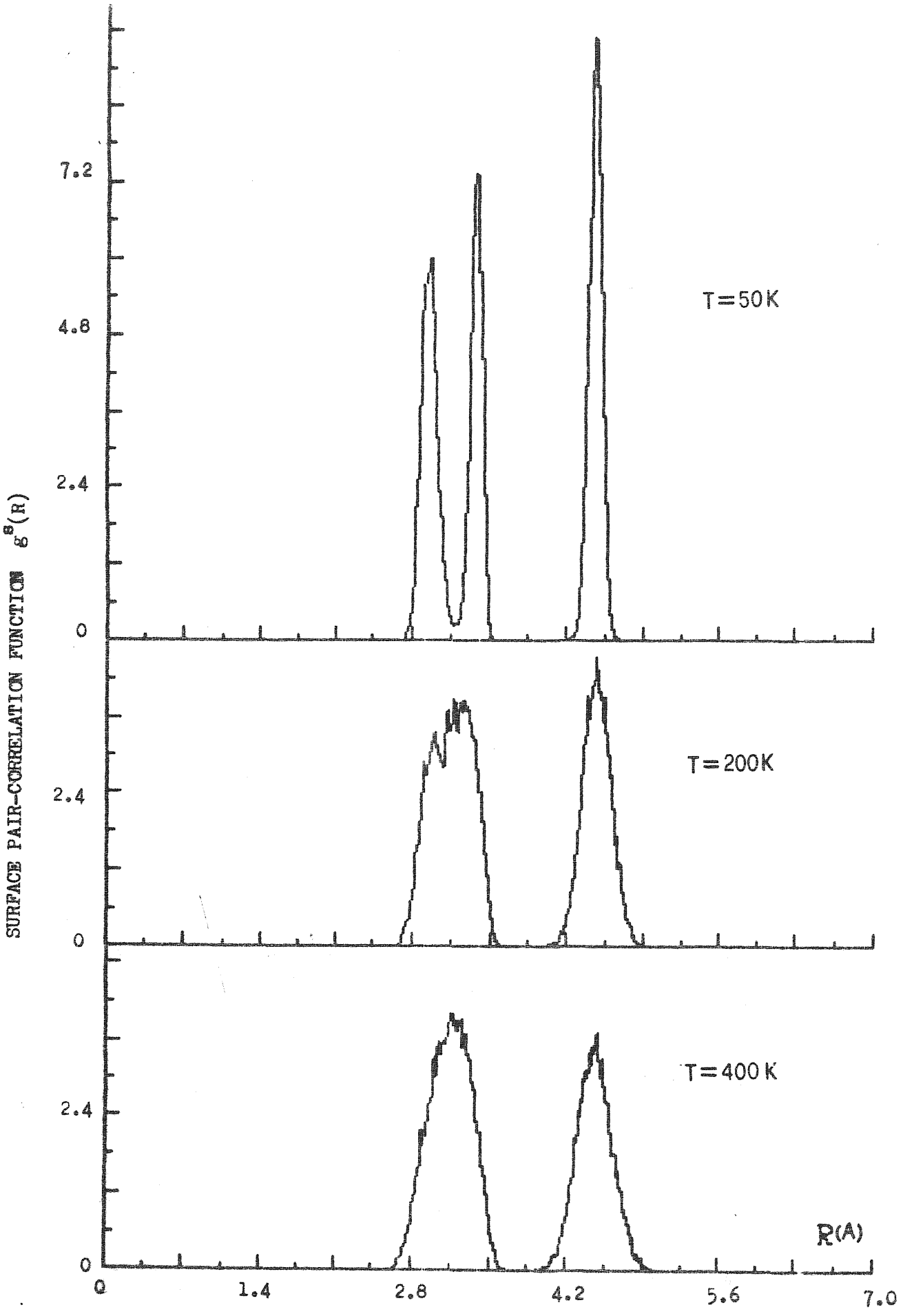

Fig. 4.7 The surface pair correlation function $g^s(R)$ obtained by using the potential "BP-B"+"SP-3" for a 8x8 sample.

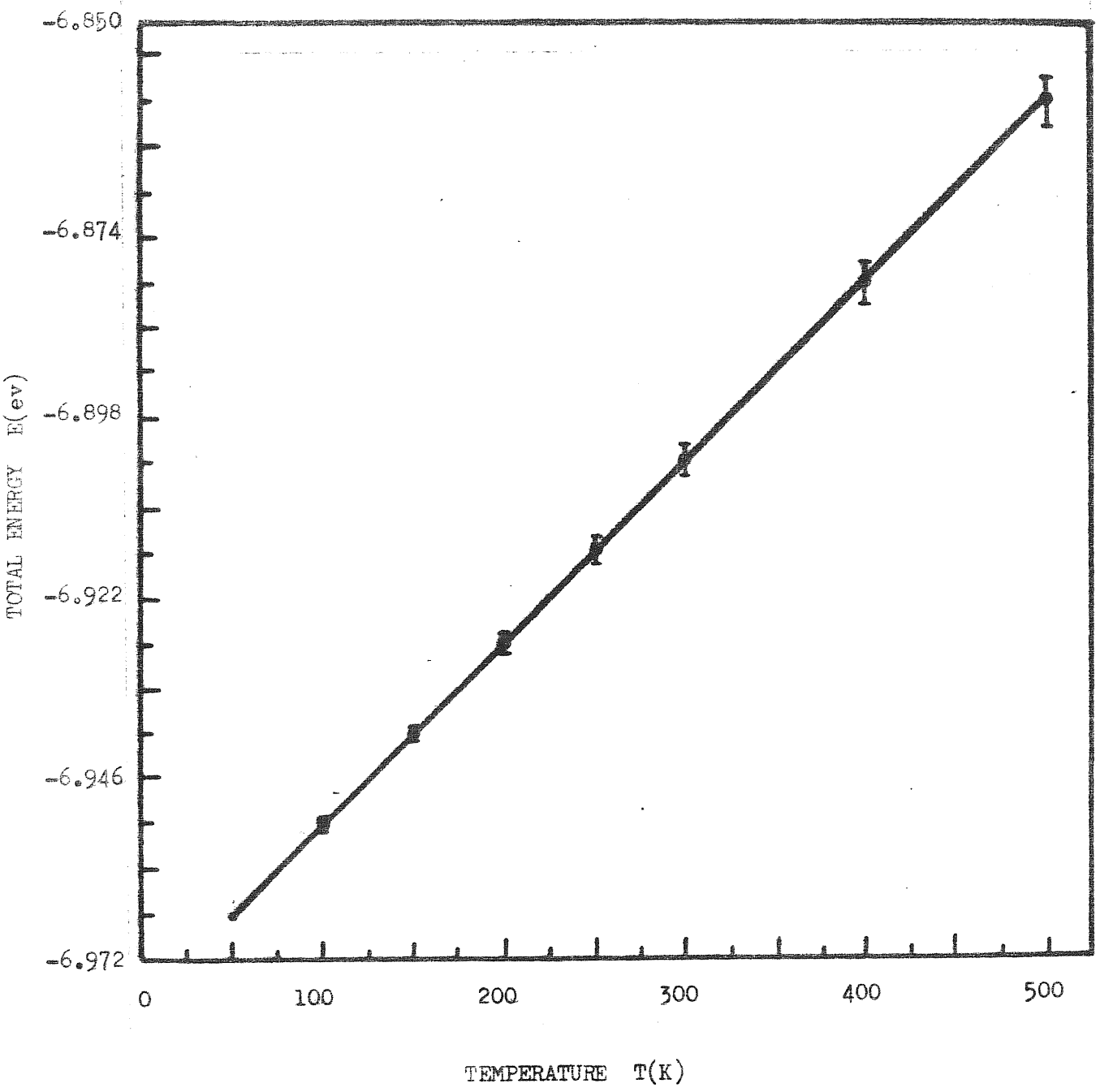

Fig.4.8 The total energy E versus temperature T, obtained by using the potential "BP-B"+SP-3" for a 8x8 sample.

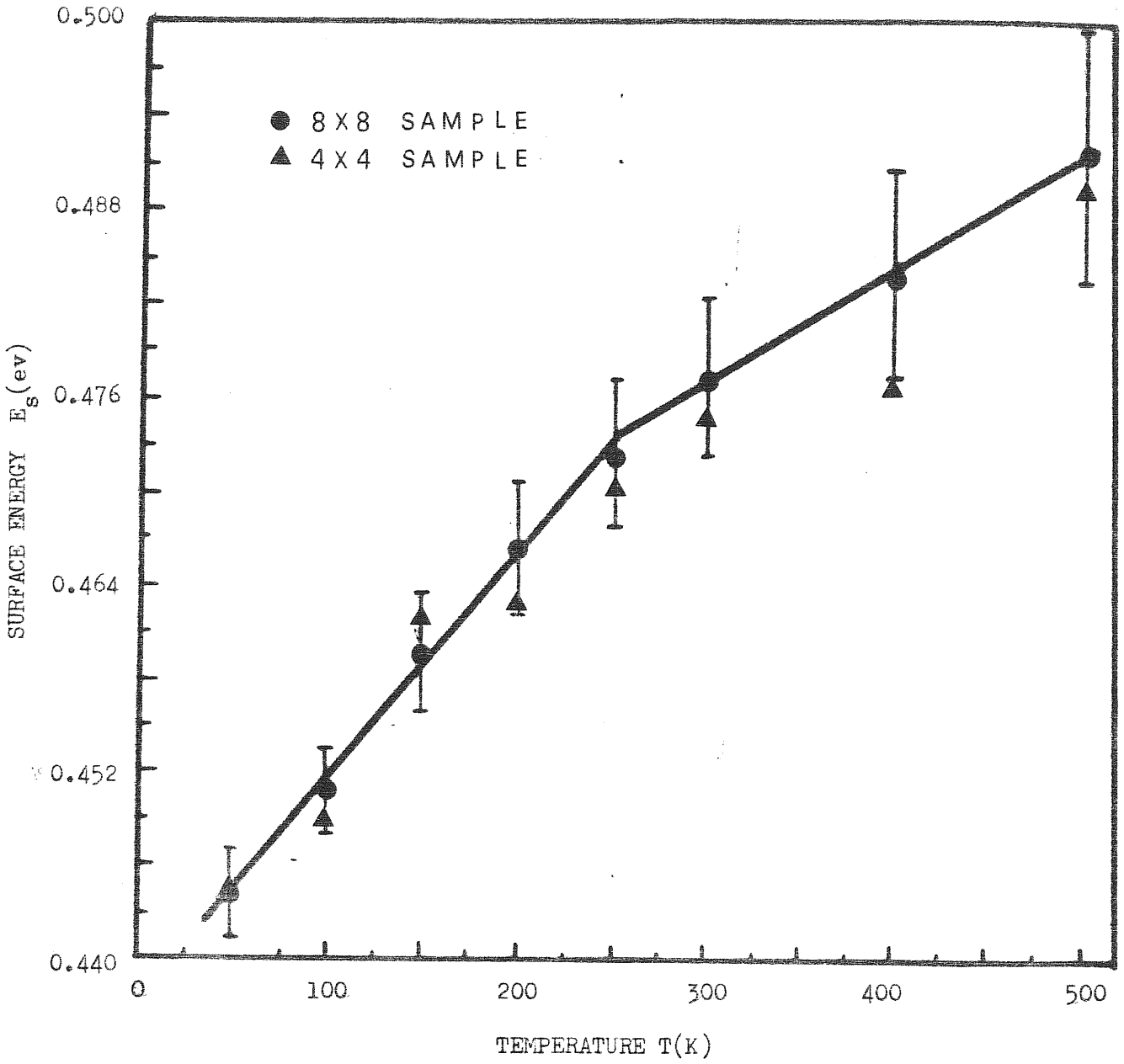

Fig. 4.9 The surface energy E_s versus temperature T obtained by using the potential "BP-B"+"SP-3" for both 8x8 and 4x4 samples.

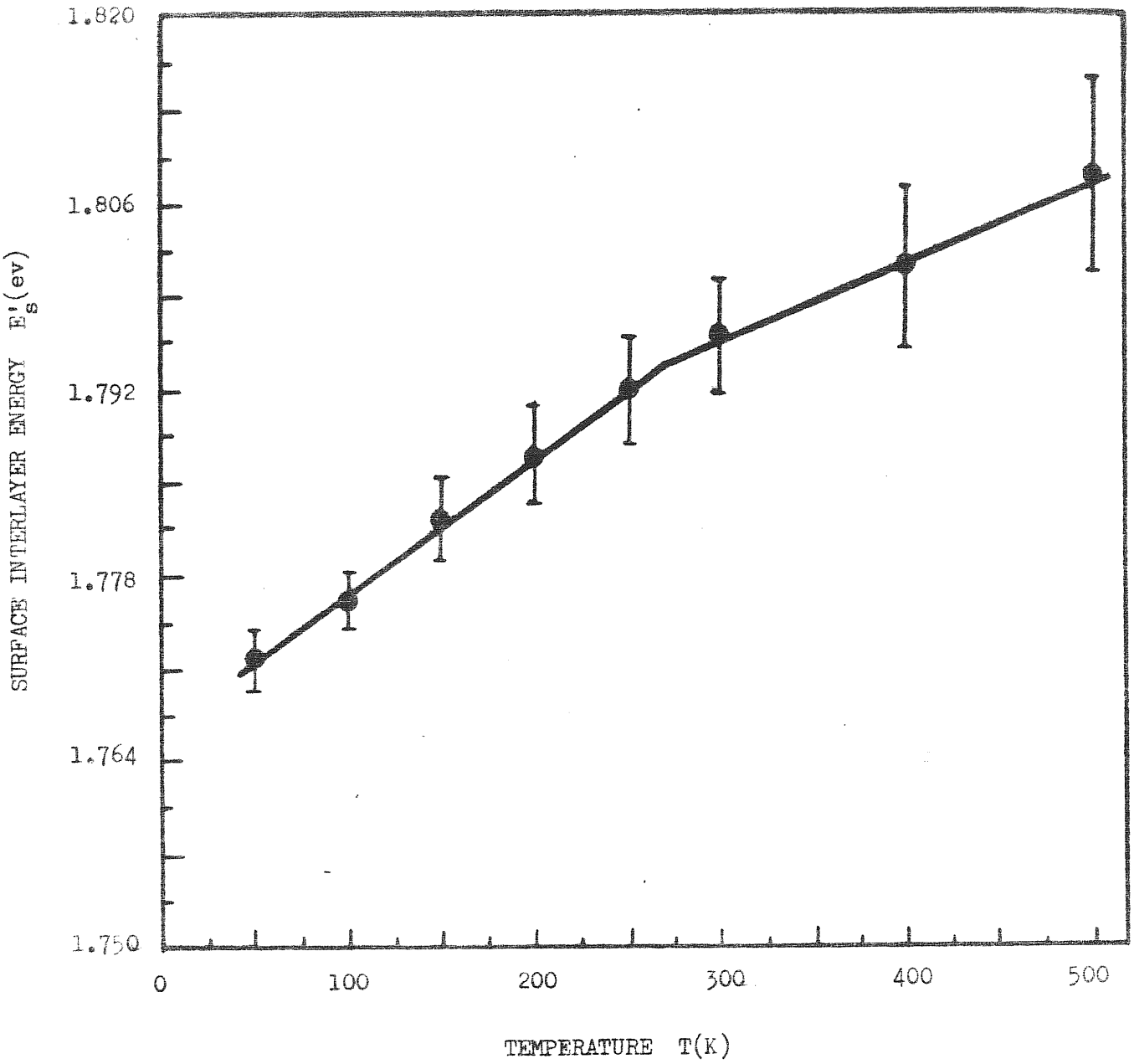

Fig. 4.10 The surface interlayer energy E_s' versus temperature T , using the potential "BP-B"+"SP-3" for a 8x8 sample.

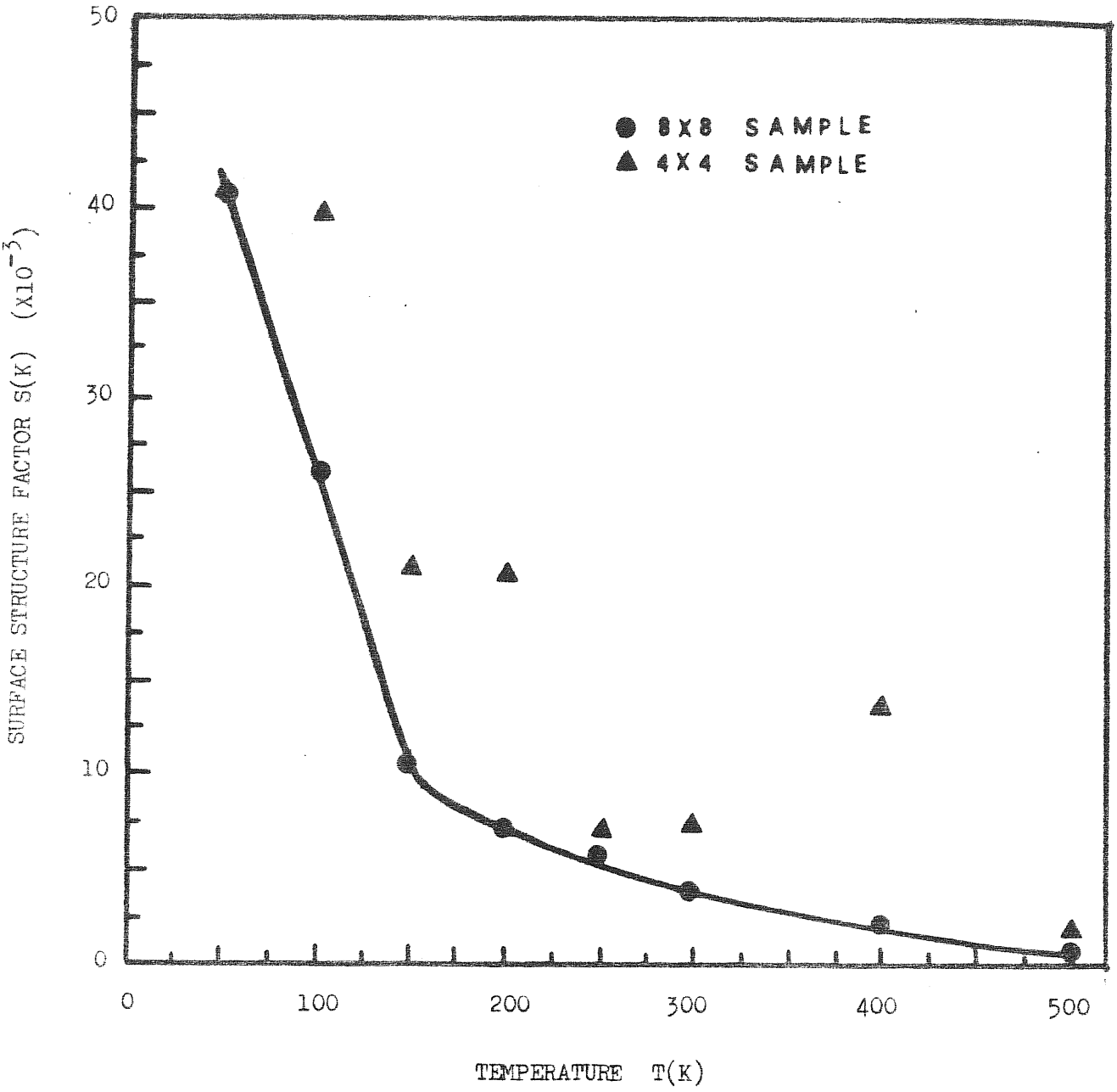

Fig. 4.11 The surface structure factor S(K) (K=(1/2,-1/2)2 /a) versus temperature T using the potential "BP-B"+"SP-3" for both 8x8 and 4x4 samples.

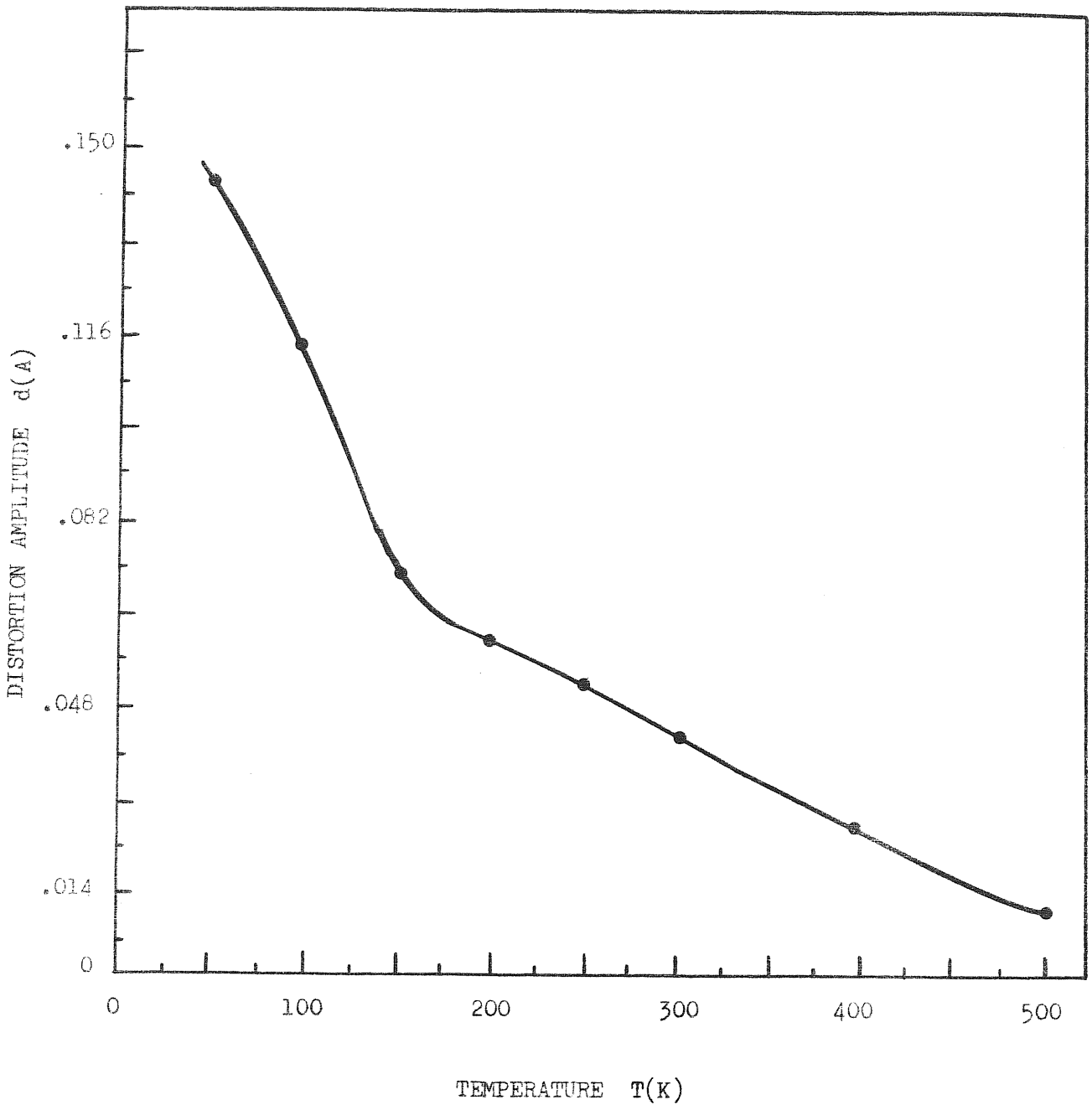

Fig. 4.12 The distortion amplitude d versus temperature T using the potential for a 8x8 sample.

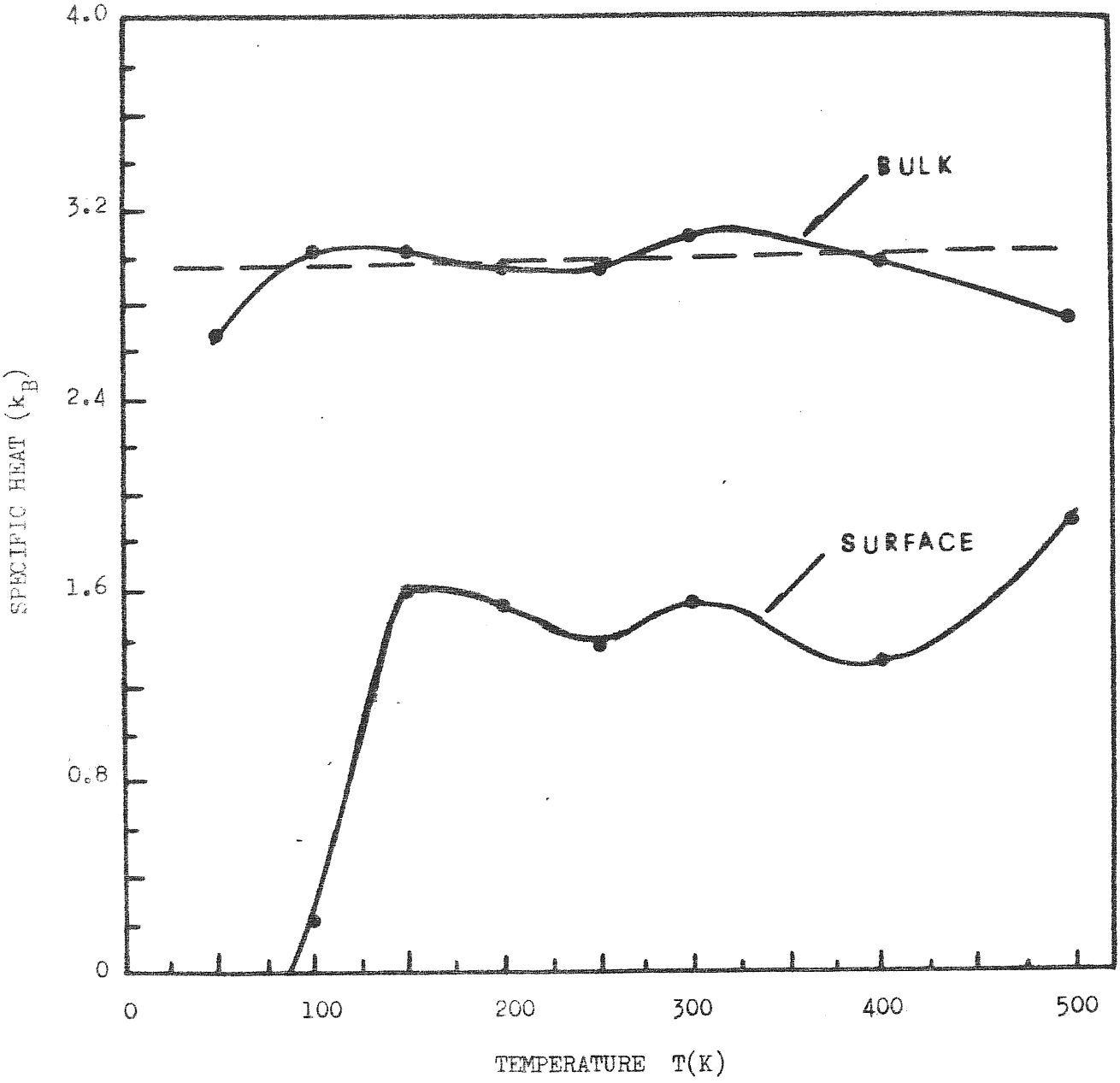

Fig. 4.13 The bulk specific heat C_v^b and the surface specific heat C_v^s versus temperature T using the potential "BP-B"+"SP-3" for a 8x8 sample.

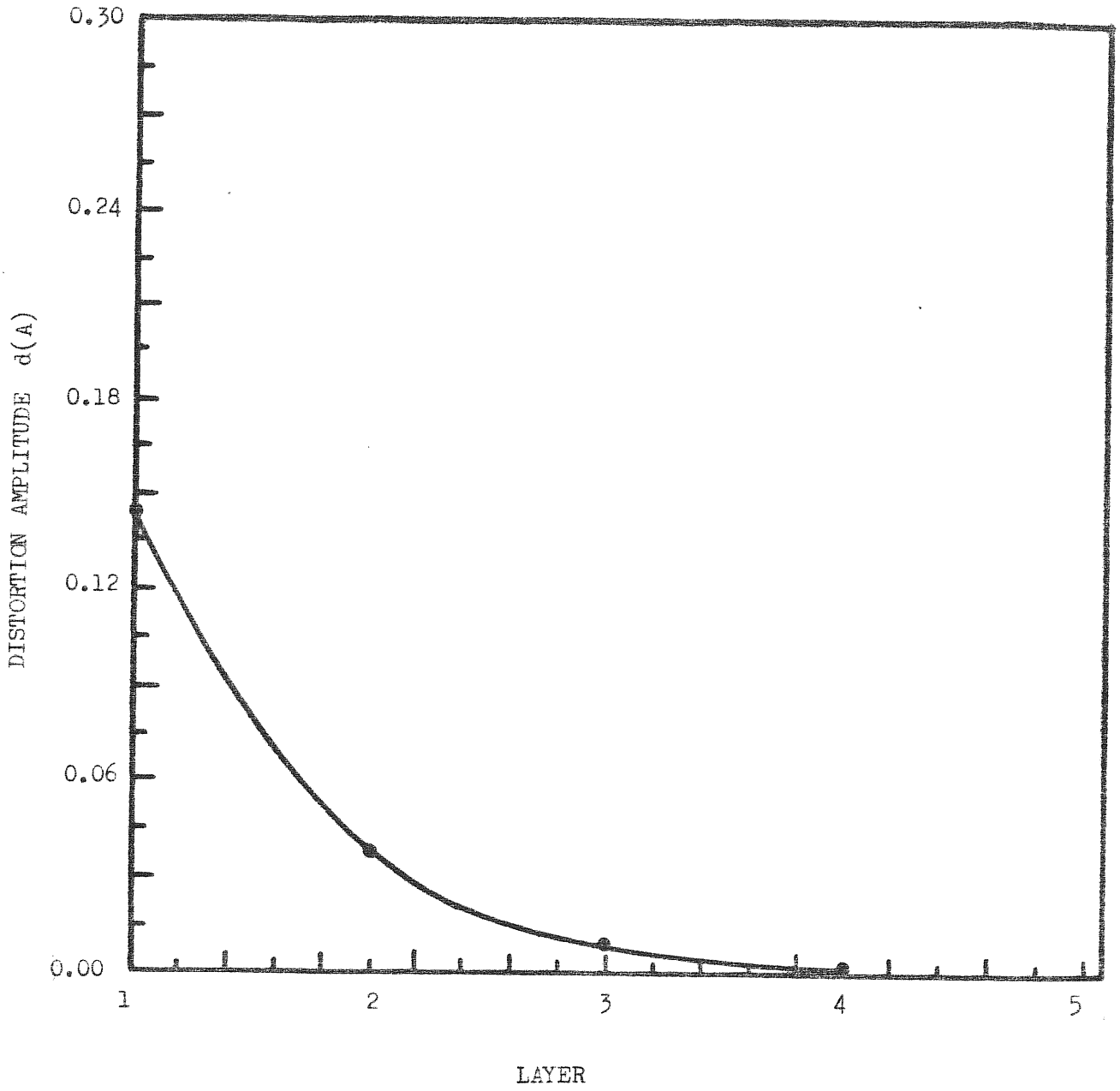

Fig. 4.14 The decaying of the distortion amplitude into the bulk.

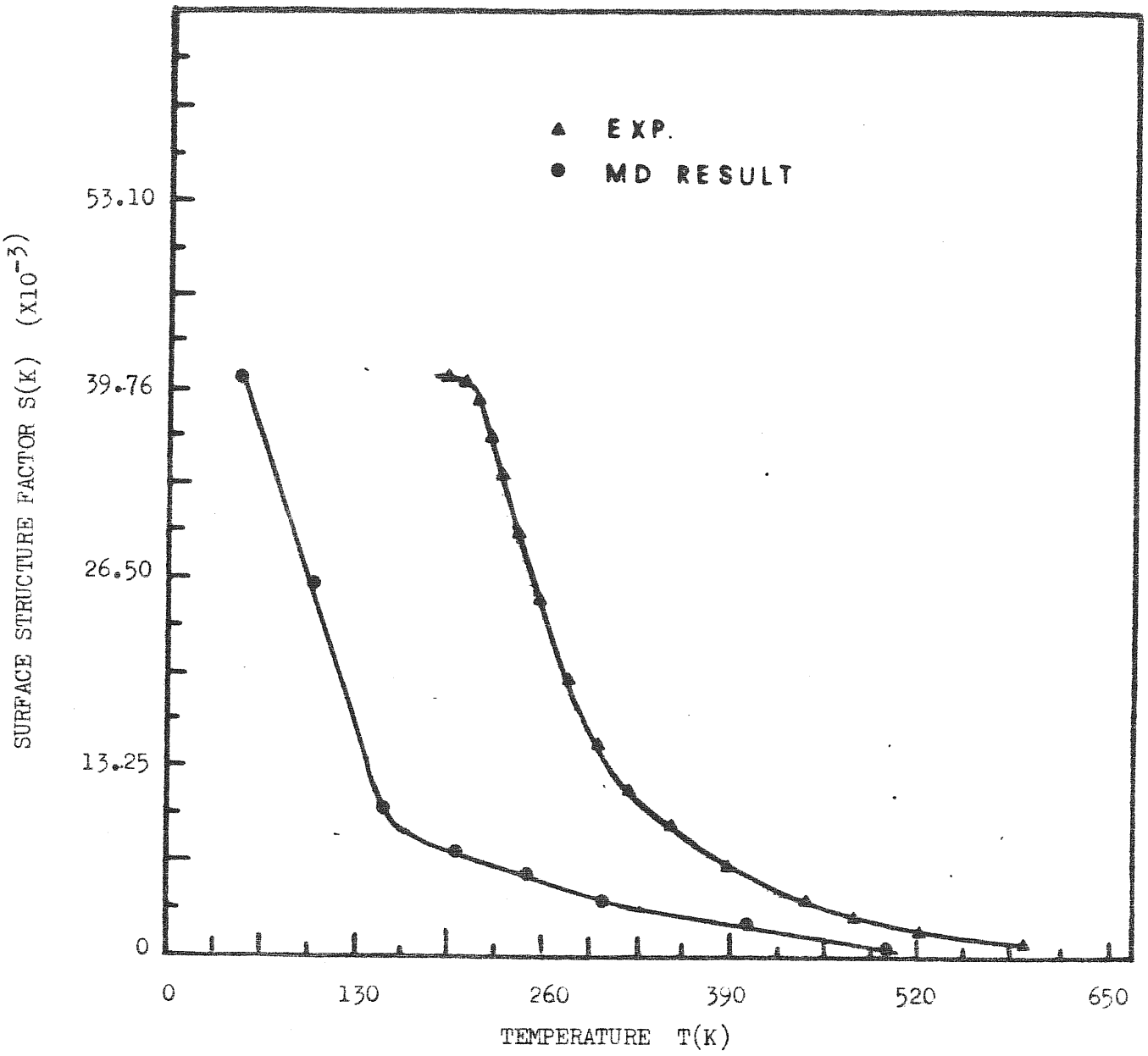

Fig. 5.1 Comparision of the MD result of surface structure factor S(K) (K=(1/2,-1/2)) to the LEED intensity of the (1/2,1/2) beam obtained by King and Thomas(1980) for the W(100) surface.

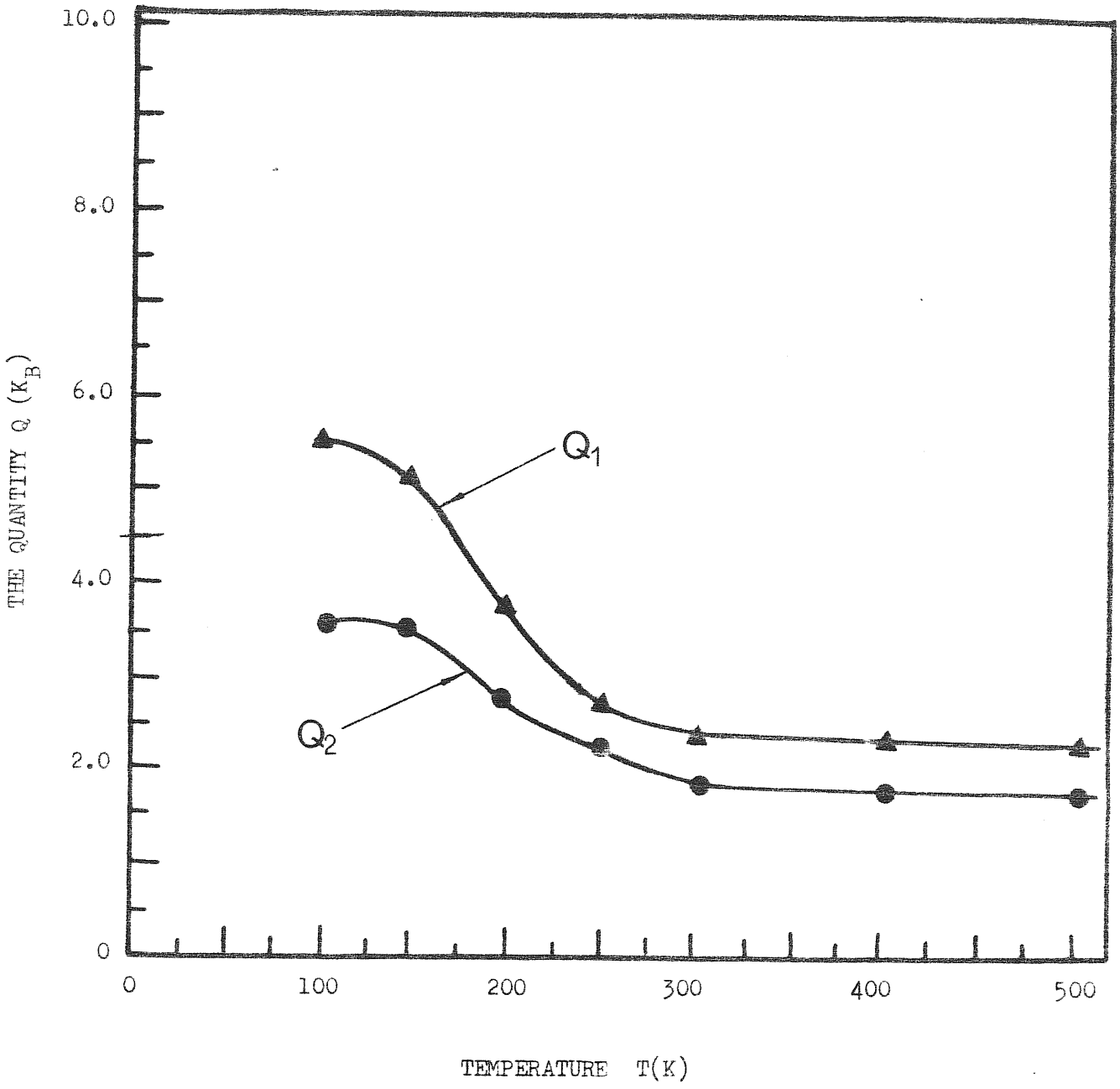

Fig. 5.2 The MD results of Q_1 and Q_2.

$$Q_1 = \frac{\langle (\Delta E_s)^2 \rangle}{K_B T^2} \quad ; \quad Q_2 = \frac{\langle (\Delta E_s')^2 \rangle}{K_B T^2}$$